Increasing heavy rainfall events in South India due to changing land use land cover

Abstract

Through an analysis of land use land cover (LULC) data for the years 2005 and 2017 from the Advanced Wide Field Sensor onboard the Indian Remote Sensing satellite, we find considerable changes in the LULC in three major states of South India, namely, Tamil Nadu, Telangana, and Kerala. This change is mainly due to increasing urbanization, in addition to the change of prevalent mixed forest into deciduous needle/leaf forest in Kerala. Motivated by this finding, we study the impact of these LULC changes over a decade on the extremity of twelve heavy rainfall events in these states through several sensitivity experiments with a convection-permitting Weather Research and Forecasting model, by changing the LULC boundary conditions. We particularly focus on three representative heavy rainfall events, specifically, over (i) Chennai (December 01, 2015), (ii) Telangana (September 24, 2016), and (iii) Kerala (August 15, 2018).

The simulated rainfall patterns of the three heavy rainfall events are found to be relatively better with the use of the 2017 LULC boundary conditions. The improvement is statistically significant in the case of the Chennai and Kerala events. On analysis of these simulations, and outputs from additional simulations we have conducted for nine other heavy rainfall events, we suggest that the recent LULC changes result in higher surface temperatures, sensible heat fluxes, and a deeper and moist boundary layer. This causes a relatively higher convective available potential energy and, consequently, heavier rainfall. We find the LULC changes in the three states, mainly dominated by the increasing urbanization in Telangana and Tamil Nadu, enhance the rainfall during the heavy rainfall events by 20% - 25%. This is the first extensive investigation of multiple and multi-regional cases over the Indian region.

1. Introduction

India is the second-largest populated country in the world, with a large fraction of population dependent on the rain-fed agriculture activities. About 70% - 80% of rainfall over India is due to the southwest monsoon, which occurs over a four-month period from June–September (JJAS). The Indian summer monsoon (ISM) covers a major portion of India, except the southeastern

region of Tamil Nadu, which receives rainfall primarily during the northeast monsoon, from October–December (OND, Rao and Jagannathan, 1953; Srinivasan and Ramamurthy, 1973).

Increasing trends in the frequency and the magnitude of extreme rainfall events during the summer monsoon have been reported in the central India during the recent decades (e.g. Goswami et al., 2006; Rajeevan et al., 2008; Pattanaik and Rajeevan, 2010; Guhathakurta et al., 2011; Singh et al., 2014; Malik et al., 2016). The number of extreme rainfall events have apparently increased by three folds in the central India during the summer monsoon season during 1950 - 2015 (Roxy et al., 2017), while a decreasing trend in the frequency of moderate events have been reported by Goswami et al. (2006); Pattanaik and Rajeevan, (2010). Various factors, such as increasing seasonal moist convective instability, strengthening of low-level monsoon westerlies and global warming, etc., have been suggested to explain the increasing extreme rainfall events in central India.

Over the tropics, particularly over the Indian sub-continent, land-surface processes constitute an important driver of the weather and climate system (e.g. Nayak and Mandal, 2012; Saha et al., 2012, 2016; Nayak et al., 2019). Several recent studies suggest, among other factors, that land use land cover (LULC) changes have an important impact on in the heavy rainfall activity over India (Pielke et al., 2011; Jain et al., 2015; Paul et al., 2016; 2018), at least at regional scales (Cook et al., 2015; Paul et al., 2016). A few case studies explored the effect of urbanization on extreme rainfall events, such as Paul et al. (2018) for the extreme rainfall event over Mumbai in India, and globally such as Niyogi et al. (2017) and Zhang et al. (2007) for extreme rainfall cases in Eastern United States and China, respectively. Indeed, urbanization is a key parameter, which often causes less evaporation, higher surface temperatures, larger sensible heat fluxes, more water-vapor mixing in the boundary layer, and higher convective available

potential energy that triggers the convection and associated rainfall (Zhang et al., 2007; Zhong and Yang, 2015; Yu and Liu, 2015).

Up-to-date, there have not been any studies on the changes in the heavy rainfall events in South India. Even though some regions of Southern India have been undergoing rapid urbanization in the last two decades (e.g. Agilan and Umamahesh, 2015; Aithal and Ramachandra, 2016; Garai and Narayana, 2018; also see our analysis in the next section), an outstanding question is whether changes in the LULC due to such rapid urbanization affect the rainfall intensity in South India. Moreover, most of related studies have been carried out for other regions, and focused only on a single event.

This question is addressed in this study through an analysis of observational rainfall datasets as well as by conducting several sensitivity studies with a convection-resolving configuration of the Weather Forecasting Research (WRF) model. While we investigate twelve heavy rainfall events, we mainly focus on the contribution of the changes in LULC through a detailed analysis of simulations pertaining to three representative heavy rainfall events in South India, one from each of the three South Indian states namely; Tamil Nadu, Telangana and Kerala (see Figure S1 for the geographical locations).

We analyze the available observed rainfall datasets in the three states, to document potential changes in the heavy rainfall events frequency and magnitude in the last two decades. The reasons for selecting these three states are as follows. The state of Kerala on the southwest Indian coast off the Arabian Sea receives copious amount of precipitation amounting to 1649.5 mm during the summer monsoon. In contrast, the state of Tamil Nadu is an eastern-coastal state off the Bay of Bengal (BoB), and as mentioned earlier, receives rainfall only during the northeast monsoon. The state of Telangana, unlike the other two states, is a land-locked state, and

relatively far off from the oceans. It receives the bulk of its annual rainfall during the summer monsoon season. While this region receives its moisture from the oceans, the importance of the LULC can be conjectured to be relatively higher owing to its location. Another distinction among the states is, because of the seasonality, the co-occurring El Niños have a propensity to exacerbate the rainfall in Tamil Nadu, unlike their detrimental effect on rainfall in the rest of India, including Telangana and Kerala (Amat and Ashok, 2018; Boyaj et al., 2018; Ashok et al., 2019). Therefore, background factors, which play a major role in defining the synoptic conditions associated with the local rainfall, can be different in these states. It will be worthwhile exploring how the heavy rainfall events in these states are affected by the LULC changes.

This manuscript is organized as follows. Section 2 describes the details of datasets, the WRF model, and methodology. Section 3 presents a brief analysis of the LULC changes in the three study regions in the recent 12 years, from 2005 to 2017. We also analyze various available observed rainfall datasets to explore potential trends in the heavy rainfall events in each state, from which we chose a representative heavy rainfall event for each state. Section 4 describes the synoptic conditions of the three selected heavy rainfall events. Section 5 discusses our results from the analyses of the LULC changes and our model simulations. Finally, the summary and conclusions are presented in Section 6.

2. Datasets and Methodology

2.1 Datasets

We analyzed the high resolution 0.25°×0.25° gridded daily rainfall datasets of India Meteorological Department (IMD) (Pai et al., 2014) over the 2000-2017 period (http://www.imdpune.gov.in/Clim_Pred_LRF_New/Grided_Data_Download.html?fbclid=IwAR

3Z_ZfZkvwjaXAAFPRSDHc4TUywjddFZYMNIJIP78vVjFR-PK1iQDVksn8). To make sure that the rainfall analyses of this high resolution dataset are not subject to any uncertainties associated with the generation of any single gridded rainfall dataset, we also examine rainfall datasets from the Tropical Rainfall Measurement Mission (TRMM) version 7 from 2000-2017 available at 0.25°×0.25° resolution (Huffman et al., 2010), the Asian Precipitation-Highly-Resolved Observational Data Integration Towards Evaluation (APRHRODITE) available at 0.25°×0.25° resolution, from 2000-2015 (Yatagai et al., 2012), the Daily Merged Satellite Gauge Rainfall (GPM) (Mitra et al., 2009) dataset available at 0.25°×0.25° resolution (ftp://ftp.ncmrwf.gov.in/pub/outgoing/). In addition, we analyzed the National Aeronautics and Space Administration (NASA) Global Precipitation Measurement Integrated Multi-Satellite Retrievals for GPM (GPM-IMERG) of level 3, version 05 available at 0.1°×0.1° resolution (Huffman, 2015). In addition, we used the fifth generation hourly gridded European Centre for Medium-Range Weather Forecasts Reanalysis (ERA5) at 0.25°x0.25° resolution datasets for validation of simulated circulation patterns (Hersbach and Dee, 2016).

2.2 WRF model

The Weather Research and Forecasting (WRF) model version 3.8.1 (Skamarock et al., 2008), which is a mesoscale numerical weather prediction system designed for atmospheric research and operational forecasting needs, is employed in this study. The WRF model predictability of heavy rainfall events over the Indian region has been ascertained in several studies (Sahany et al., 2010; Hari Prasad et al., 2011; Bhanu Kumar et al., 2012; Srinivas et al., 2018; Chawla et al., 2018, Viswanadhapalli et al., 2019). For this study, the model has been configured with two-way interactive nested three domains with horizontal outer-to-inner resolutions of 18, 6 and 2 km. The regions of the first and second domains are common for all three heavy rainfall events; the

innermost domain is zoomed over the respective regions of each heavy rainfall event. The selected physics options include, the Goddard Ensemble scheme for microphysics (Tao et al., 2016), Dudhia for short-wave radiation scheme (Dudhia et al., 1989), Rapid Radiation Transfer Model (RRTM) for long-wave radiation (Mlawer et al., 1997), Yonsei University (YSU) non-local scheme (Hong et al., 2006) for planetary boundary layer and NOAH scheme (Tewari et al., 2004) for land surface processes. The Kain-Fritsch (KF) scheme (Kain, 2004) is used for the cumulus convection in the first and second domains. Adhering to the high resolution of the inner domains, no implicit cumulus scheme is used for the inner domain. The initial and lateral boundary meteorological conditions for the model are obtained from the National Centers for Environmental Prediction-Final Analysis (NCEP-FNL) data available for every six hours at 1°x1° resolution (NCEP, 2000). Our simulations for each heavy rainfall event start at 0000 UTC of the day prior to the heaviest rainfall day of the event, as catalogued by the IMD. For example, in the case of Chennai heavy rainfall event, as per the IMD, the peak rainfall occurred on 01 December, 2015. Our corresponding simulations are initiated at 0000 UTC of 30 November, 2015.

2.3 Methodology

We analyze heavy rainfall events and their changes in the recent two decades during the primary rainfall season, i.e. summer monsoon season for the Telangana and Kerala states, and the northeast monsoon for Tamil Nadu. We identify heavy rainfall events, from the gridded IMD rainfall datasets, following the IMD classification (http://imd.gov.in/section/nhac/termglossary.pdf). Accordingly, the heavy rainfall events are defined as those events for which the rainfall amount lies between ≥35.6 mm/day to ≤124.4 mm/day. In addition to the daily IMD gridded rainfall data sets, two other observed daily gridded

rainfall datasets, APHRODITE and TRMM, were also chosen for further analysis. At every grid point, we compute the linear trends in seasonal heavy rainfall days, and the 99 percentile of rainfall magnitude.

Based on the analysis results of the IMD dataset, we identify three heavy rainfall events - one for each of the three states of the Tamil Nadu, Telangana and Kerala, as representative cases that receive detailed attention. The selected events respectively occurred (i) on 01-December, 2015 over Tamil Nadu, (ii) 24-September, 2016 over Telangana, and (iii) 15-August, 2018 over Kerala. We conduct various sensitivity experiments with the WRF model to evaluate the potential contribution of the recent LULC changes to the extremity of each of these representative events. Due validation of the important simulations was carried out through a comparison with the observational datasets. In this study, the peak rainfall hours/stage, for each of these three representative events, are defined as the three to four contiguous heaviest rainfall hours, as deciphered from the time series of area-averaged GPM rainfall time-series; the area-averaging is done over the state in question. Next three hours after the peak rainfall are designated as the decaying stage. Similarly, we define the three hours before the peak stage as the developing stage, unless mentioned otherwise.

The LULC dataset from the Moderate Resolution Imaging Spectroradiometer (MODIS) with 20 categories (Table 1) based on the year 2001 (Ran et al., 2010; Bhati and Mohan, 2018) are used in the standard WRF model configuration. In addition, an option to use the United States of Geological Survey (USGS) LULC conditions of 1995 is also available. Notably, a new LULC dataset for the over Indian continent was obtained from the Advanced Wide Field Sensor (AWiFS) aboard the Indian Remote-Sensing Satellite (IRSP6), (https://bhuvan-app3.nrsc.gov.in/data/download), which was launched by the Indian Space Research

Organization (ISRO). These LULC datasets with 24 categories (Table 1) are generated at three resolutions of 5m (~9 km), 2m (~3.5 km) and 30s (~0.9 km) on annual basis from 2005 till 2017 (Biswadip et al., 2014). Using the MM5 model, Badrinath et al., (2012) suggested that the track of the Aila cyclone was better simulated over Indian region with the ISRO LULC relative to that with the USGS LULC. Unnikrishnan et al., (2016) reported that an updated ISRO LULC in the dynamic model gives the better weather prediction over India. More recently, Sahoo et al. (2020) have carried out multiple ensemble simulations of the extreme event over Uttarakhand, which occurred in 2013. This study suggests that using the 2013 ISRO LULC, as compared to the 2005 ISRO LULC, results in a better simulation of the extreme rainfall event.

As the categories of the LULC from ISRO data, developed mainly for the Indian region, are similar in-terms of number and types to those of the USGS LULC datasets, the ISRO LULC datasets can be used for simulations over India without any serious technical challenges. Equally important is the suggestion from the various case studies (e.g. Badrinath et al., 2012, Unnikrishnan et al., 2016; Sahoo et al., 2020) that the simulations with concurrent ISRO LULC datasets exhibit better fidelity related to those with the MODIS and/or USGS LULC. Given that these datasets are available from 2005, they provide a potentially ideal dataset to carry out sensitivity experiments in order to evaluate the implication of the local LULC changes for the any changes in extremity of the heavy rainfall events over South India. Therefore, our sensitivity experiments with the WRF model mainly comprise of using the ISRO LULC over the study region of Indian sub-continent (6°N - 40°N, 65°E - 100°E), in addition to the ‘control experiments with the MODIS LULC, as detailed in the next paragraph.

In case of each representative heavy rainfall event we had identified in section 4, we carry out three experiments, by changing the LULC datasets. These are, (i) the control

experiment, henceforth referred to as the 'MODIS' experiment, characterized by the LULC datasets of MODIS, (ii) the 'Old-ISRO' experiment with the ISRO LULC dataset for the year 2005, and (iii) the 'New-ISRO' experiment, with the LULC datasets of the year 2017. We also carry out similar simulations for nine more heavy rainfall events to generate relevant statistics to understand the potential influences of the recent changes in the LULC on the heavy rainfall events.

We plan to carry out simulations at a relatively high horizontal resolution of 2 km; it is worth recalling a study by Baskarao et al. (2010). This study suggests that, for improved simulations of synoptic disturbances in the Indian region at a high horizontal resolution of 1~4 km, the vertical resolution should also be commensurately high. From this context, we carry out several preliminary sensitivity simulations with two vertical resolutions, namely, the standard 30 vertical levels that are default in WRF, and a higher 51 vertical levels we designed, comprising of 30 vertical levels in the lower troposphere (from the surface to 500 hPa), and the remaining 21 in the middle and upper troposphere (above 500 hPa to 10 hPa). We carry out six complementary simulations sensitivity tests to ascertain the best suitable vertical resolution. The first three simulations, with the default vertical resolution of WRF differ from one another by the choice of the LULC datasets. Based on the LULC dataset used, and the vertical resolution implemented, these experiments are referred to as MODIS-30, Old-ISRO-30, and New-ISRO-30. The corresponding complementary experiments with the 51 vertical levels are named similarly lines. As indicated by the Figure S2, the simulation with the higher vertical resolutions suggests a better fidelity in capturing the observed features (Figure S2g, h, and i).

It must also be mentioned that all the in-situ and/or satellite observations-based gridded rainfall datasets used for our analysis are at coarse horizontal resolutions of about 10-25 km,

while our model simulations are carried out at a high resolution of 2 km. In this context, the broad similarities we seek between the observations and model simulations are the location of the peak rainfall, orientation and distribution of the rainfall. In addition, the simulated circulation is compared with the corresponding reanalysis dataset from the ERA5.

The statistical significance of the trends in the observed frequency of the heavy rainfall events and those in the 99 percentile of rainfall magnitude, in each region, are evaluated by a one-tailed Student's t-distribution. The significance of correlations, etc., is evaluated using a one-tailed Student's t-test.

3. Changes in heavy rainfall events and LULC in South India

Figures 1 and 2 show the distributions of linear trend in seasonally aggregated number of heavy rainfall days over the period of 2000-2017 in the three states of Tamil Nadu, Telangana and Kerala, and the corresponding trends in the 99 percentile of seasonal rainfall magnitude, from multiple rainfall datasets such as IMD, APHRODITE, and TRMM. Analysis of the IMD and APHRODITE datasets indicates an increase in the 99 percentile of rainfall magnitude over the northern Tamil Nadu during the northeast monsoon season, and northern part of Telangana as well as central part of Kerala during summer monsoon season (Figure 2). The 99 percentiles of the seasonal rainfall amounts, from the IMD and APHRODITE datasets show a significant (95% confidence level) trend over the northern part of Tamil Nadu during the northeast monsoon, and Telangana and central part of Kerala during the summer monsoon. The TRMM dataset, however, do not show a significant trend in the seasonal 99 percentiles of the rainfall over Telangana and Kerala. The positive trend observed in the frequency of heavy rainfall events in all three states (except in the TRMM dataset over Telangana) is, however, statistically not significant.

The distributions of LULC over the three different states of Tamil Nadu (Figures 3a, d, g), Telangana (Figure 3b, f, h), and Kerala (Figure 3c, e, i) show an expansion of urbanization in recent periods. A significant reduction is observed in the crop/grass land in all states, which turned into a dry crop land and pasture. Water bodies and crop/wood lands have expanded in Tamil Nadu. Mixed shrub land/grass land became barren/sparsely vegetation in Telangana, and a broad green fraction of mixed forests turned into deciduous needle/leaf forest over the Kerala.

The above results suggest that the heavy rainfall events in all three states are increasing in recent decades in potential conjunction with significant changes in the local LULC. However, at this stage, it is difficult to come up a final conclusion whether the LULC changes have unequivocally enhanced the rainfall. To this end, we carry out various sensitivity experiments with the WRF, as stated earlier.

4. Synoptic conditions of the heavy rainfall events

4.1 The Chennai event

Chennai (13.5°N, 80.1°E), the fourth largest city in India and capital of Tamil Nadu located in the southeast coast of India with an estimated population of 8.7 million (Census, 2011). Chennai, as well as most of Tamil Nadu, experienced a heavy rainfall event during 26 November - 02 December, 2015, reaching its peak rainfall above 300 mm/day on 01 December 2015 (Figure 4). Several studies and reports have provided the details of the synoptic conditions for this event (India. Met. Dept. Rep., 2015; Chakarborty, 2016; Mishra, 2016; Narasimhan et al., 2016; Srinivas et al., 2018). As per these papers, a slow-moving low-pressure system was observed during 27 November - 02 December, 2015 off the coast of Tamil Nadu over southwest BoB, which resulted in heavy rainfall at 12°N – 14°N, 79°E – 80.1°E over the north coastal Tamil

Nadu and the neighborhood regions. Based on several WRF sensitivity experiments Boyaj et al. (2018) claimed that the extremity of the event is due to the concurrent Mega El Niño as with the warming trend in the sea surface temperature off the coast of Tami Nadu.

4. 2 The Telangana event

The state of Telangana experienced heavy rainfall of about 250 mm/day on 24 September 2016, which was 107% above the whole climatological rainfall for the month of September. As per the IMD reports, the maximum rainfall occurred over the northwest parts of Telangana, and was mainly associated with the formation of a well-marked low-pressure system over the central BoB and the adjoining area of coastal Andhra Pradesh, with cyclonic circulation extending from the surface up to 7.6 km on 22 September 2016. This surface low pressure system moved towards the interior of Andhra Pradesh. The system was then located further west over Vidarbha and Telangana regions on 23 and 24 September 2016, contributing to the heavy rainfall over the north-western parts of Telangana during 24 - 25 September 2016. The highest amount of rainfall of 390 mm was recorded at a station called Armoor (18.79°N, 78.29°E) on 24 September, 2016, with 320 mm and 270 mm of rainfall recorded at the neighboring Machareddy and Kamareddy on 25 September, 2016. The details of synoptic and rainfall distributions are available at

https://www.aphrdi.ap.gov.in/documents/Trainings@APHRDI/2017/7_July/DRR/A%20case%20study%20on%20monsoon%20rainfall%20over%20Andhra%20Pradesh%20state%20in%20relation%20to%20synoptic%20systems.pdf.

4. 3 The Kerala event

The state of Kerala, located on the southwest coast of India, experienced prolonged severe flood during 01 - 19 August, 2018, the heaviest ever recorded in 100 years. This heavy rainfall (50

mm/day to 480 mm/day) caused enormous damage and about 500 causalities. A detailed diagnostic study of this event was carried out by Viswanadhapalli et al. (2019) through an analysis of observations and high-resolution WRF model simulations. The present study states that several major factors, specifically, a strong monsoon flow along with the formation of an offshore vortex, a transport of mid-tropospheric moisture from the Arabian Sea, and a convective low vertical shear of horizontal wind were instrumental for the heavy rainfall. The heavy rainfall occurred in two spells over 7 - 10 August and 14 - 18 August, 2018, with a southward movement of rainfall bands from the northern mountain regions to the coastal areas of Kerala. The highest amount of rainfall during the first spell concentrated over the northeast mountain regions and a second spell with the maximum over central and south-central of Kerala. Heavy rainfall of 450 mm occurred during 09 - 10 August at Pookot station. Similarly, the Valparai station received about 950 mm of rainfall during 14 - 15 August, 2018.

5. Results and discussion

5.1 Sensitivity to vertical resolution

This section reports results from the preliminary experiments conducted to ascertain the vertical resolution. To validate our simulations, we focus on specific features such as the location of the peak rainfall, orientation, magnitude and asymmetries of the rainfall distribution, among others features, which should be broadly captured by the relatively coarse observations as well. The model simulations (Figure S2) generally exhibit improved fidelity with the observed heavy rainfall with 51 vertical levels configuration. For example, the Chennai heavy rainfall simulated with 30 vertical levels resolution is oriented in the east-west direction (Figures S2d-f) and most of the rainfall magnitude concentrated over the ocean regardless of the used LULC data, which is different from that in the observations (Figures S2a-c). The corresponding simulations with 51

vertical levels resolution are, however, oriented south-north (Figures S2g-f) and the rainfall magnitude concentrated over the coastal land area, in agreement with the observations. The fine features of the model simulations are not artefacts of high resolution, as was evidenced by a companion study (Srinivas et al., 2018), which suggested that the features captured by the interpolated station observations data for the Chennai heavy rainfall event in question have been well simulated (Figure not shown). Therefore, in this paper, we present our results from the simulations carried out with the 51 vertical levels configuration model.

5.2 Impact of changes in LULC on heavy rainfall events

In this section, we present results from our nine simulations that examine the sensitivity of the simulated representative events, to different choices of the LULC, all of course generated with 51 vertical levels. Various panels in Figures 4 to 6 show the results of rainfall from nine different model simulations; also shown in these figures are the corresponding observed rainfall distributions from three different observed datasets.

In the case of the Chennai heavy rainfall event, using a high resolution Automatic Weather Gauge network over Chennai as well as rainfall derived from the Doppler weather radar data at the Chennai city, Srinivas et al. (2018) suggested that the observed rainfall over Chennai exhibited a high spatial variability with isolated heavy rainfall within the range of few kilometers. Figures 2a and 2b of Srinivas et al. (2018) are based on the automatic weather stations around Chennai and the IMD Doppler Weather Radar on 01 December 2015, the day of the maximum rainfall. These demonstrate (Figure not shown) that the 24-hour accumulated rainfall on this day extended southward from 13°N, ~12.7°N, at about 79.9°E. The IMD gridded rainfall datasets also show (Figure 4c) a high concentration of rainfall along the east coast of the Tamil Nadu, with a maximum between 12°N - 14°N, 79.5°E - 80.1°E, along a north-south

oriented rainfall band. Similar patterns are seen (Figure 4a, b) from the other two observations datasets (TRMM and GPM-IMERG), with slight spatial differences, The analysis of high resolution observations by Srinivas et al. (2018) gives a good opportunity to ascertain the fidelity of our simulations at high resolution. The corresponding simulation of 24-hour accumulated rainfall on 01 December, 2015 with the New-ISRO LULC simulation (Figure 4f) captures the location and the north-south orientation (shown with arrow mark) of the heaviest 24-hour rainfall and asymmetries (Figure 2a and 2b, respectively of Srinivas et al., 2018) reasonably well simulation with the New-ISRO LULC. However, the simulations with the MODIS and Old-ISRO LULC (Figure 4d, e) instead show a southeast-northwest orientation of the aforementioned rain band. All three simulations, though, simulate about 20%-25% less rainfall that as reported by the Doppler weather radar as well as the automatic weather stations over Chennai.

For the Telangana heavy rainfall event, the peak 24-hour accumulated rainfall was concentrated over the north-western part of Telangana (Figure 5a-c) on 24 September, 2016. The area and magnitude of peak rainfall is slightly different across the three observational datasets (Figure 5a-c). The corresponding simulation with the New-ISRO LULC over Telangana state (Figure 5f) is comparable with the IMD observations in terms of the magnitude and area of the heavy rainfall. The simulated heavy rainfall with New-ISRO LULC is concentrated at 18.7°N and 78.2°E in conformation (shown with plus "+" mark) with the IMD observations (Figure 5c). It must, however, be mentioned that the simulated 24-hour accumulated rainfall with the New-ISRO LULC (Figure 5f) is an underestimate when compared with the corresponding GPM-IMERG rainfall estimate (Figure 5b). The MODIS and Old-ISRO LULCs (Figure 5d, e) simulations, to some extent, match better with the GPM-IMERG rainfall datasets in this case.

Figures 6a-c show the spatial heavy rainfall patterns over the Kerala state from the observational datasets of TRMM, GPM-IMERG and IMD. One can see that the heaviest rainfall is concentrated in the central and southern parts of Kerala on 15 August, 2016 (Figure 6b and c), with a general westward extension of the rainfall into the Arabian Sea. All the three observational datasets look qualitatively similar (Figures 6a-c), though the magnitude of the maximum rainfall is much weaker in the TRMM rainfall. We find from Figures 6b and 6c that the maximum zone of rainfall (shown in circle) extended from around 10.9°N till 9.1°N in a narrow northwest-southeast direction (shown in arrow mark). The corresponding simulations in general capture the general areal extent of the rainfall, including its extension into the Arabian Sea from the Kerala coast. However, the simulated the maximum rainfall is slightly weaker in than observations (Figure 6c) around 10.5°N (Figures 6d, e, and f). Importantly, the simulation with the New-ISRO LULC (Figure 6f) can be seen to extend up to 9.1°N, unlike the other two simulations.

We have now computed the correlations between the hourly GPM-IMERG rainfall on the peak rainfall day, and that from relevant simulations, for the three representative events (Figure 7). The correlations are computed for eight hours (the peak hour and seven hours prior to that). Our analysis suggests that the areal extent of regions with positive correlations (0.72) that are significant at 95% confidence level is higher with the New-ISRO LULC. This particularly applies to the rainfall maxima regions. While ascertaining the significance levels for correlation values, we have confirmed that the observed hourly rainfall, over the eight hours over which the correlations are calculated, are subject to autocorrelation at many grid points for each of the case. Based on the resultant number of degrees of freedom, is coincidentally found to be 4 for all cases. Thus, a correlation magnitude of 0.72 (0.60) is significant at 95% (90%) confidence level

from a one-tailed Student's t-test. All these suggest that the model performance improved with the updated LULC.

A comparison of the time-series area-averaged simulated rainfall from each of the three representative events with the corresponding time series from the GPM-IMERG rainfall (Figure not shown) suggests that the timing and duration of the maximum rainfall and that of the decaying phase, particularly in case of Chennai and Telangana events, are captured marginally better with the New-ISRO LULC lower boundary conditions. .

Based on our results so far, we can state that various simulated rainfall characteristics of the three representative heavy rainfall events such as the spatial distribution and asymmetries somewhat better simulated using the New-ISRO LULC, relative to those with the MODIS and Old-ISRO LULCs.

5.3 Simulated moisture, vorticity, zonal and vertical wind analysis

The available moisture in the atmosphere is a major factor in for any heavy rainfall event (Brimelow and Reuter, 2005; Pathak et al., 2017; Yang and Smith, 2018). The dynamical and physical processes that facilitate the transport of the moisture are also important factor. A co-location of the maxima of simulated vertically integrated moisture, low level vorticity, and upward vertical motion with the location of the observed rainfall is a strong indication of the fidelity of the model. In this context, it is useful to examine the implications of any changes in the LULC to the moisture pathways that contribute to the heavy rainfall. To this end, we have analyzed the simulated vertically integrated (integrated from surface to 300 hPa) moisture fluxes and their transport, these results are shown in Figures 8, 10 and 12. We also analyze the

corresponding various kinematics to understand the spatial patterns of the large-scale circulation (Figures 9, 11, and 13) for all three heavy rainfall events with different LULCs.

Our analysis of the hourly evolution of the vertically integrated moisture (VIM) from the ERA5 reanalysis for all three heavy rainfall events (Figures 8d, 10d, and 12d) suggest that the moisture convergence regions are mostly smooth in ERA5, likely due to the relatively coarser resolution. In contrast, the corresponding model results are associated with asymmetries. Notwithstanding this, the large-scale directions of the moisture transport vectors (Figures 8, 10, and 12) as well other features such as the zones of moisture convergence in the observations and corresponding model simulations show relatively similar patterns.

We present a brief analysis of the moisture availability, and its transport during the peak of the Chennai heavy rainfall event, both from the ERA5 datasets and our simulations, in Figure 8. From the ERA5 datasets, we find the moisture from the adjoining BoB being transported towards the land region of the northern part of Tamil Nadu during the peak rainfall hours of the (Figure 8d) Chennai heavy rainfall event. The simulations (Figures 8a-c) broadly reflect these low level wind moisture transport features. However, the spatial distributions of the VIM over Tamil Nadu from the all simulations (Figures 8a-d) are different from one another. During the peak rainfall hours, the VIM is concentrated around 12.5°N – 13.5°N in all the simulations (Figures 8a-d). Notably, the New-ISRO LULC simulation indicates a maximum zone of VIM oriented north-south over the coast along northern part of Tamil Nadu, and the adjoining BoB (Figure 8c). This is in agreement with not only the location and orientation of the simulated rainfall during the peak hours (Figure 4f), but to some extent with those of the observed rainfall (Figures 4a-c). The other two experiments with the MODIS and Old-ISRO LULC, on the other hand, simulate the VIM more over the inland. Furthermore, the corresponding simulated zonal

wind, relative vorticity, and upward motion at 850 hPa during the peak rainfall hours of Chennai heavy rainfall event are shown in Figure 9. The experiments with MODIS and Old-ISRO LULC datasets (Figure 9a and b) simulate relatively weak low level magnitudes of vorticity and vertical wind relatively over the north coastal Tamil Nadu as compared to that over more inland, which is associated with the shift of vertical moisture into inland (Figures 8a and b). The New-ISRO LULC experiment (Figure 9c) simulates a broad region of vertical wind concentrated over the coastal area, which conform to the simulated as well as observed highest rainfall (Figures 4b and c).

Figures 10 and 12 show the reanalyzed as well as simulated VIM, and moisture transport for the Telangana and Kerala heavy rainfall events during the peak rainfall time, respectively. The corresponding low level vorticity and circulation are shown in Figures 11 and 13, respectively. The ERA5 reanalysis datasets show two discrete spatial maximum of VIM over Telangana at 19°N - 20°N, 79°E, and 18°N - 19°N, 77.8°E regions during the peak rainfall hours in the ERA5 dataset (Figure 10d). The VIM is better simulated by the New-ISRO LULC in these regions (Figure 10c). The second peak at 19°N - 20°N, 79°E is not so well captured in the simulations with the MODIS and Old-ISRO LULCs (Figures 10a and 10b). Theses simulations also overestimate the areal extent of low level vorticity and vertical velocity maximums (Figure 11a and b) as compared to the New-ISRO LULC (Figure 11c), and apparently hence the higher observed heavy rainfall zone (Figure 5b).

For the Kerala heavy rainfall event, the VIM and its transport as deciphered from ERA5 dataset during the peak hour are shown in Figures 12d, and those from simulations in Figure 12a-c. The VIM is observed to be maximized at north and south of the coastal regions of Kerala during the peak rainfall hours, as per the ERA5 dataset (Figure 12d). The simulated vertically

integrated moisture in the experiment with the New-ISRO LULC shows the simulated VIM extending from central through south coastal Kerala, but with an extension from into the Arabian Sea westward (Figure 12c). The northern peak of the VIM is not adequately simulated. Notwithstanding this, this simulated aspect is matching with the spatial rainfall maximum during the peak, which was observed over the South coastal Kerala (Figures 6b and c). The meridional width of the simulated VIM on the coastal Kerala in the corresponding of Old-ISRO LULC, just as the simulated rainfall is narrower than observed (Figure 12b). The MODIS LULC experiment is marginally better (Figure 12a). The simulated vertical wind and vorticity patterns are similar in all the respective LULC simulations for Kerala heavy rainfall event (Figures 13a-c).

The area averages of simulated vertical winds with height during the starting, peak and decaying stages of heavy rainfall hours of the three heavy rainfall events are shown in Figure 14. The vertical winds profiles over the three regions clearly show that a gradual increase in the vertical wind between the 800 hPa to 300 hPa levels with time. The maximum upward motion of the storm sustains for about 4 hours in all the cases, after which it starts decreasing, indicating the terminal stage of the life cycles of each of the systems. These higher vertical velocities at these levels are crucial for the vertical pumping of the moisture and deepening of the storm, thus for the heavy rainfall. These patterns are to some extent represented by the New-ISRO LULC based simulation relative to the other two experiments.

The above analysis suggests that the WRF model with New-ISRO LULC provides somewhat better realistic simulations of each of the three heavy events over the South India, as compared to the other two simulations with older LULC datasets. In the next sub-section, we investigate changes in the simulated physical processes associated with an updated

representation of the LULC dataset, which result in relatively a better replication of the extremity of the rainfall as well as its temporal evolution.

5.4 Implications of changes in LULC/Urbanization on the boundary layer processes during the heavy rainfall events

In the context of various studies that have suggested that the LULC changes resulted in increasing heavy rainfall events elsewhere through a change in the boundary layer processes and interactions (e.g. Zhang et al., 2007; Niyogi et al., 2017), we explore in detail the changes in the boundary layer processes associated with the changes in the LULC, which contributed to the extremity of the three heavy events we discussed above. To do so, we analyze the differences in the simulated atmospheric variables such as the surface temperature, sensible heat flux, planetary boundary layer height (PBLH), water vapor, convective available potential energy (CAPE), and water vapor mixing ratio resulting from the Old-ISRO and New-ISRO LULC experiments, these results are presented in Figures 15-17.

For all the three heavy events, the New-ISRO LULC configuration simulates surface temperatures that are warmer by about 0.2°C to 0.5°C than those obtained with the Old-ISRO simulations (Figures 15a, 16a, and 17a). Such increases in surface temperatures result in increases in the corresponding sensible heat fluxes by about 20-40 W/m^2 (Figures 15b, 16b, and 17b). These higher surface temperature and sensible heat flux are associated with a deeper boundary layer height of about 100~150 meters (Figures 15c, 16c, and 17c), higher water vapor mixing ratios of about 0.2~0.5 g/kg^{-1} (Figures 15f, 16f, 17f), and high CAPE values around 300~500 J/kg (Figures 15e, 16e, and 17e). The regions with lower surface temperature and sensible heat fluxes are, in contrast, associated with lower water vapor at the surface (Figures 15d, 16d, and 17d).

Importantly, for all three heavy rainfall episodes, the regions with the higher surface temperature, sensible heat fluxes, boundary layer height, CAPE and water vapor mixing ratio are (Figures 15-17) seen with an increase in the urban/sub-urban zone (Figure 3c, 3f and 3i). The spatial distributions of the rainfall in the three cases also clearly indicate that the regions of heavy rainfall are located in/adjacent to the urban regions. This suggests that increasing urbanization in the peninsular India results in increased surface temperatures, sensible heat flux, PBLH, water vapor mixing ratio and CAPE, which, when released, results in the increased rainfall extremity (Figures 4, 5, 6 and S3). These results are in agreement with several recent case studies (e.g. Miao et al., 2011; Wan and Zhong, 2014; Yang et al., 2014; Zhong and Yang, 2015; Yu and Liu, 2015). This clearly suggests that the recent changes in LULC need to be accounted for in the advanced high-resolution mesoscale models reliably to predict the heavy rainfall events.

To further substantiate our findings, in addition to the three representative heavy events that we have discussed in detail so far, as mentioned earlier, we have performed several numerical simulations of the additional the earlier-mentioned nine additional heavy rainfall events that had occurred over the three states (3 events over each state). The simulated area-average rainfall from these experiments, shown as the percentage of the corresponding observed IMD rainfall in Figure S3, varies from the observations by 20% - 25%. In contrast, the results from the Old-ISRO LULC experiments deviate substantially from the IMD observations. From this context, the simulations with the New-ISRO LULC can be deemed to be more realistic. We carry our further analysis to ascertain this point. We investigated heavy rainfall events from the IMD datasets, the area over which maximum rainfall, the peak day for each of the 12 considered cases (including the three sample cases), extends. We have then computed the area-averaged rainfall

over these regions of maximum rainfall (Table S1). The corresponding values from all the simulations are also included. We have then calculated the correlations of the observational values with the corresponding simulations. While the correlation with the Old-ISRO LULC is 0.43, significant only at 90% confidence level, the corresponding correlation in the case of the New-ISRO LULC is a high 0.7 and significant at 99.95% level. This strongly demonstrates that the use of the updated (New-ISRO) LULC has improved the simulation of heavy rainfall events.

Further analysis of the simulations for these nine heavy events also suggest that, just a for the three representative cases we presented in detail (Table S2), increasing urbanization has resulted in higher surface temperatures, larger sensible heat fluxes, and deeper boundary layer. These changes in the boundary layer characteristics, mainly due to increased urbanization, can be deemed to have eventually led to increased extremity of the higher amount of rainfall of about 20% - 25%, as can be deciphered from the difference in simulated rainfall associated with the changed LULC (Figure S3). Further, the analysis of these simulations clearly confirms that the changes in the LULC are critical for an accurate simulation, and potentially prediction, of a heavy rainfall event.

This suggests that a realistic, updated LULC is important for the optimal simulations of heavy rainfall events, and presumably their prediction. More importantly, these results also clearly indicate that the recent changes in the local LULC are playing an important role in the local synoptic weather conditions over the three states.

6. Summary and conclusions

Significant increases in the frequency and the magnitude of heavy rainfall events have been reported over India in the last few decades. These events often cause tremendous damage such as wiping off crops, landslides, floods, loss of human lives and property, etc. Several case studies suggest that land use land cover (LULC) changes associated with urbanization have led to increasing heavy rainfall events as well as their intensity, as for example, in China (Zhang et al., 2007), and in USA (Niyogi et al., 2017), in addition to India (Paul et al., 2018).

Importantly, during the recent decades, the urbanization has been rapidly increasing in the South Indian states. Through the analysis of observed datasets such as gridded observed rainfall datasets from of IMD, TRMM, and GPM-IMERG, and carrying out several simulations with convection permitting WRF model. The current study explores the potential impact of LULC changes on the heavy rainfall events, which occurred over the three southern states of India, namely, Telangana, Tamil Nadu, and Kerala the last two making up the southernmost region of the Indian peninsula. Of these, Tamil Nadu, a state in the southeastern India, off the coast of the Bay of Bengal, receives rainfall mainly during the northeast monsoon season from October-December. In contrast, the southwestern state of Kerala receives its rainfall during the southwest monsoon. The state of Telangana is located to the north of the above two states, and is a land-locked state. It receives rainfall mainly during the summer monsoon season. Of late, several heavy rainfall events have been reported in these states (e.g. Visawnathapalli et al., 2019; Srinivas et al., 2018). Interestingly, one common factor across these states is an apparent urbanization as implied by the increasing industrial activity and migration to cities.

Therefore, in this study, we analyzed the available LULC data for the Indian region from the Advanced Wide Field Sensor (AWiFS) onboard the Indian satellite IRS P6 (IRS P6) for two years 2005 and 2017. An analysis of the IRSP6 LULC changes suggests that urbanization has

increased over the Hyderabad (Telangana), Chennai (Tamil Nadu) mega-city regions in addition to other LULC changes. The mixed forest turned into deciduous needle/leaf forest over Kerala, in addition to increased urbanization. Such an LULC changes motivated us to explore whether the increasing urbanization has contributed to the extreme intensity of the rainfall events.

To this end, we identified twelve heavy rainfall events, which have occurred in the last decade or so. Then, for each of these events, we carried out several numerical sensitivity experiments with the Weather Forecasting Model (WRF). In all our experiments, we implemented a triple nesting configuration with a horizontal resolution of 2 km for the inner grid covering the state in question and neighborhood regions in order to capture fine features such as the rain bands, magnitude and location of the heavy rainfall events. Based on sensitivity experiments with different number of vertical layers, all our simulations with 51 vertical levels enable a realistic simulation of the heavy rainfall distributions.

For the sake of brevity, we focused on three representative heavy rainfall events. The details of the three representative heavy rainfall events have been well documented. These occurred, specifically, over (i) Tamil Nadu, mainly the Chennai city, with a peak on December 01, 2015, (ii) Telangana with a peak on September 24, 2016, (iii) and over Kerala with a peak on August 15, 2018. Several numerical experiments were performed using the WRF model in order to ascertain whether the recent LULC changes in these states have contributed to each of these three heavy events.

Our numerical simulations suggest that the spatial rainfall patterns and asymmetries of heavy rainfall events are relatively better reproduced when the new LULC datasets of 2017 vintage provided by ISRO was used as a lower boundary condition instead of the default MODIS LULC of year 2001 vintage or even the ISRO 2005 LULC datasets. The simulations with the

newest LULC lower boundary conditions facilitate realistic simulations of the observed heavy rainfall as well as that of fine features such as the asymmetric nature of rainfall distribution, concentrated rainfall over isolated regions, and meridional/zonal extension of rainfall, etc. The increase of the model resolution allowed resolving the urban effects more accurately and further the asymmetries of heavy rainfall and higher intensity are likely occurred due to the accurate representation of LULC in the model.

The analysis of the simulations of twelve heavy events, including the three focused events show that urbanization produces higher surface temperatures, larger sensible heat fluxes, a deeper boundary layer, less water vapor, more water-vapor mixing in the boundary layer, and hence more convective available potential energy. The conducted sensitivity experiments suggest that about 20%-25% of the rainfall in the recent heavy rainfall events over South India can be attributed to the changes in LULC/increased urbanization in the last decade. Our results also imply that up-to-date LULC boundary conditions, along with increased vertical levels, may also lead to an enhancement in the predictive skills of heavy rainfall events over South India.

Acknowledgements

The authors thank the India Meteorological Department (IMD) for providing gridded rainfall dataset. We also acknowledge all data providers (ISRO, TRMM, APHRODITE, GPM, ERA5 and NCEP) that made their datasets available for this study. Dr. K. Srinivasarao (NRSC) support in the usage of the IRSO LULC datasets is particularly acknowledged, and Dr. K. Nagaratna (IMD, Begumpet, Hyderabad) for providing synoptic information of the Telangana event. The first author is thankful to KAUST for providing a student visiting research fellowship to carry out this research. All model simulations were carried out on the KAUST supercomputing facility

Shaheen. Also acknowledge Council of Scientific and Industrial Research (CSIR) for the Senior Research Fellowship (SRF).

References

Agilan, V., Umamahesh, N.V. (2015) Detection and attribution of non-stationarity in intensity and frequency of daily and 4-h extreme rainfall of Hyderabad, India. Journal of Hydrology, 530, 677-697.

Aithal, B.H., and Ramachandra, T.V. (2016) Visualization of Urban Growth Pattern in Chennai Using Geoinformatics and Spatial Metrics. J. Indian Soc. Remote Sens. 44, 617–633.

Amat, H.B., and Ashok, K. (2018) Relevance of Indian Summer Monsoon and its Tropical Indo-Pacific Climate Drivers for the Kharif Crop Production. Pure Appl. Geophys, 175, 3, p1221.

Ashok, K., Feba, F., and Tejavath, Ch. (2019) The Indian summer monsoon rainfall and ENSO Mausam, 70(3):443-452.

Badarinath, K.V.S., Mahalakshmi, D.V., and Ratna S.B. (2012) Influence of Land Use Land Cover on Cyclone Track Prediction-A Study During Aila Cyclone. Open Atmos. Sci. J., 6, 33–41, doi:10.2174/18742823012-06010033.

Bhanu Kumar, O.S.R.U., Suneetha,P., Ramalingeswara Rao, S., Satya Kumar, M. (2012) Simulation of Heavy Rainfall Events during Retreat Phase of Summer Monsoon Season over Parts of Andhra Pradesh. International Journal of Geosciences, 3-4, doi:10.4236/ijg.2012.34074.

Biswadip, G. (2014) IRS-P6 AWiFS derived gridded land use/land cover data compatible to Mesoscale Models (MM5 and WRF) over Indian Region. NRSC Technical Document No. NRSC-ECSA-ACSGOCT-2014-TR-651, 1–11.

Boyaj, A., Ashok, K., Ghosh S., Devanand, A., Dandu, G. (2018) The Chennai extreme rainfall event in 2015: the Bay of Bengal connection. Climate Dynamics, 50(7–8):2867–2879.

Brimelow, J.C., Reuter, G.W. (2005) Transport of atmospheric moisture during three extreme rainfall events over the Mackenzie River Basin. J Hydrometeorol 6:423–440.

Chakraborty, A. (2016) A synoptic scale perspective of heavy rainfall over Chennai in November 2015. Curr Sci,1–21.

Chawla, I., Osuri, K., Mujumdar, P., Niyogi, D. (2018) Assessment of the Weather Research and Forecasting (WRF) model for simulation of extreme rainfall events in the upper Ganga Basin. Hydrol. Earth Syst. Sci, 22, 1095–1117.

Cook, B.I., Shukla, S.P., Puma, M.J., and Nazarenko, L.S. (2015) Irrigation as an historical climate forcing. Climate Dynamics, 44, 1715–1730. doi.org/10.1007/s00382-014-2204-7.

Dudhia, J. (1989) Numerical study of convection observed during the Winter Monsoon Experiment using a mesoscale two–dimensional model. J. Atmos. Sci, 46, 3077–3107. doi:10.1175/1520-0469(1989)046<3077:NSOCOD>2.0.CO;2.

Garai, D., and Narayana, A.C. (2018) Land use/land cover changes in the mining area of godavari coal fields of southern India. The Egyptian Journal of Remote Sensing and Space Sciences. 2, 375–381.

George Huffman. (2015) GPM IMERG Late Precipitation L3 Half Hourly 0.1 degree x 0.1 degree V05, Greenbelt, MD, Goddard Earth Sciences Data and Information Services Center (GES DISC), Accessed, 10.5067/GPM/IMERG/3B-HH-L/05.

Goswami, B.N., Venugopal, V., Sengupta, D., Madhusoodanan, M.S., and Xavier, P.K. (2006) Increasing trend of extreme rain events over India in a warming environment. Science, 314, 1442–1445. doi:10.1126/science.1132027.

Guhathakurta, P., Sreejith O.P., and Menon, P.A. (2011) Impact of climate change on extreme rainfall events and flood risk in India. J. Earth Syst. Sci, 120(3), 359–373.

Hariprasad, D., Venkata Srinivas, C., Venkata Bhaskar Rao, D., Anjaneyulu, Y. (2011) Simulation of Indian monsoon extreme rainfall events during the decadal period 2000–2009 using a high resolution mesoscale model. Adv Geosci A6:31–48.

Hersbach, H., and Dee, D. (2016) ERA5 reanalysis is in production, ECMWF Newsletter 147, ECMWF, Reading, UK.

Hong, Song You, Yign Noh, Jimy Dudhia. (2006) A new vertical diffusion package with an explicit treatment of entrainment processes. Mon. Wea. Rev., 134, 2318 2341.doi:10.1175/MWR3199.1.

Huffman, G., Adler, R., Bolvin, D., and Nelkin, E. (2010) The TRMM Multi-Satellite Precipitation Analysis (TMPA), in: Satellite Rainfall Applications for Surface Hydrology, edited by: Gebremichael, M. and Hossain, F., 3–22, Springer Netherlands, doi:10.1007/978-90-481-2915-7.

IMD, (2015) India Meteorological Department (https://metnet.imd.gov.in/imdnews/ar2015.pdf). Accessed on 6 November, 2019.

Jain, S.K., and Kumar, V. (2012) Trend analysis of rainfall and temperature data for India. Curr Sci, 102(1) 37–49.

Kain John, S. (2004) The Kain–Fritsch convective parameterization: An update. J. Appl. Meteor., 43, 170–181. doi:10.1175/1520-0450(2004)043<0170:TKCPAU>2.0.CO;2.

Malik, N., Bookhagen, B., and Mucha, P.J. (2016) Spatiotemporal patterns and trends of Indian monsoonal rainfall extremes. Geophys Res Lett, 43(4):1710–1717. doi:10.1002/2016GL067841.

Miao, S.G., Chen, F., Li, Q.C., and Fan, S.Y. (2011) Impacts of urban processes and urbanization on summer precipitation: A case study of heavy rainfall in Beijing on 1 August 2006, J. Appl. Meteorol. Climatol.,50 (4), 806– 825.

Mishra, A.K. (2016) Monitoring Tamil Nadu flood of 2015 using satellite remote sensing. Nat Hazars. 82(2):1431–1434.

Mitra, A.K., Bohra, A.K., Rajeevan, M.N., Krishnamurti, T.N. (2009) Daily Indian precipitation analysis formed from a merge of rain-gauge data with the TRMM TMPA satellite-derived rainfall estimates. Journal of the Meteorological Society of Japan, 87A. pp. 265-279. ISSN 0026-1165, doi.10.2151/jmsj.87A.265.

Mlawer., Eli. J., Steven, Taubman, J., Patrick, Brown, D., Iacono, M.J., and Clough, S.A. (1997) Radiative transfer for inhomogeneous atmospheres: RRTM, a validated correlated–k model for the longwave. J. Geophys. Res., 102, 16663–16682. doi:10.1029/97JD00237.

Narasimhan, B., Murty Bhallamudi, S., Mondal, A., Ghosh, S., and Mujumdar, P. (2016) Chennai floods 2015 – A rapid assessment. Interdisciplinary Centre for Water Research, Indian Institute of Science, Bangalore, 49p.

Nayak, H.P., Palash Sinha., Satyanarayana, A.N.V., Bhattacharya. A., Mohanty, U.C. (2019) Performance Evaluation of High-Resolution Land Data Assimilation System (HRLDAS) Over Indian Region. Pure Appl. Geophys, 176: 389. https://doi.org/10.1007/s00024-018-1946-2.

Nayak, S., and Mandal, M. (2012) Impact of land use and land cover change on temperature trends over Western India. Current Science, 102(8), 1166–1173.

National Centers for Environmental Prediction/National Weather Service/NOAA/U.S. Department of Commerce (2000), NCEP FNL Operational Model Global Tropospheric Analyses, continuing from July 1999, https://doi.org/10.5065/D6M043C6, Research Data Archive at the National Center for Atmospheric Research, Computational and Information Systems Laboratory, Boulder, Colo.

Niyogi, D., Lei, M., Kishtawal, C., Schmid, P., and Shepherd, M. (2017) Urbanization Impacts on the Summer Heavy Rainfall Climatology over the Eastern United States. Earth Interact, https://doi.org/10.1175/EI-D-15-0045.1.

Pai, D.S., Sridhar, L., Rajeevan, M., Sreejith, O.P., Satbhai, N.S., Mukhopadyay, B. (2014) Development of a new high spatial resolution (0.25° × 0.25°) long period (1901–2010) daily gridded rainfall dataset over India and its comparison with existing data sets over the region. Mausam 65(1):1–18.

Pathak, A., Ghosh, S., Martínez, J.A., Domínguez, F., and Kumar, P. (2017) Role of Oceanic and Land Moisture Sources and Transport in the Seasonal and Interannual Variability of Summer Monsoon in India, J. Climate, 30, 1839–1859.

Pattanaik, D.R., and Rajeevan, M. (2010) Variability of extreme rainfall events over India during southwest monsoon season. Meteorol. Appl, 17, 88–104.

Paul, S., Ghosh, S., Mathew, M., Devanand, A., Karmakar, S., and Niyogi, D. (2018) Increased spatial variability and intensification of extreme monsoon rainfall due to urbanization. Sci Rep, 8(1):3918.

Paul, S., Ghosh, S., Oglesby, R., Pathak, A., Chandrasekharan, A., and Ramsankaran, R. (2016) Weakening of Indian summer monsoon rainfall due to changes in land use land cover. Sci. Rep, 6,32,177.

Pielke Sr, R., Pitman, A., Niyogi, D., Mahmood, R., McAlpine, C., Hossain, F., Fall, S. (2011) Land use/land cover changes and climate: modeling analysis and observational evidence. Wiley Interdisciplinary Reviews: Climate Change. 2, 828–850.

Prakash, S.M.C., Sathiyamoorthy, V., Gairola, R.M. (2013) Increasing trend of northeast monsoon rainfall over the equatorial Indian Ocean and peninsular India. Theor Appl Climatol, 112, 1, 185–191.

Rajeevan, M., Bhate, J., and Jaswal, A.K. (2008) Analysis of variability and trends of extreme rainfall events over India using 104 years of gridded daily rainfall data. Geophys. Res. Lett, 35, L18707. doi:10.1029/2008GL035143.

Ran, L., Pleim, J., Gilliam, R. (2010) Impact of high resolution land-use data in meteorology and air quality modeling systems. In: Steyn GD, Rao TS (eds) Air pollution modeling and its application, vol XX. Springer Netherlands, Dordrecht, pp 1–108.

Rao, D.V.B., Hari Prasad, D., Srinivas, D., and Anjaneyulu, Y. (2010) Role of vertical resolution in numerical models towards the intensification, structure and track of tropical cyclones. Marine Geod, 33, 338–355.

Roxy, M.K., Ghosh, S., Pathak, A., Athulya, R., Mujumdar, M., Murtududde, M., Terray, P., and Rajeevan, M. (2017) A threefold rise in widespread extreme rain events over central India. Nat. Commun. 8, 708.

Saha, S.K., Dirmeyer, P.A., and Chase, T.N. (2016) Investigating the impact of land-use land-cover change on Indian summer monsoon daily rainfall and temperature during 1951–2005 using a regional climate model. Hydrology and Earth System Sciences, 20, 1765–1784.

Saha, S.K., Halder, S., Rao, A.S., and Goswami, B.N. (2012) Modulation of ISOs by land–atmosphere feedback and contribution to the interannual variability of Indian summer monsoon. J. Geophys. Res., 117, D1301. doi:10.1029/2011JD017291.

Sahany, S., Venugopal,V., Nanjundiah, R.S. (2010) The 26 July 2005 heavy rainfall event over mumbai: numerical modeling aspects. Meteorology and Atmospheric Physics. 115-128.

Sarika Jain. (2015) WRF model analysis of land-surface processes over Jaipur Region. International Journal of Scientific & Engineering Research, Volume 6, Issue 5, ISSN 2229-5518.

Singh, D., Tsiang, M., Rajaratnam, B., and Diffenbaugh, N.S. (2014) Observed changes in extreme wet and dry spells during the South Asian summer monsoon season. Nat. Clim., 4(6):456–461. doi:10.1038/nclimate2208.

Skamarock, W.C., Klemp, J.B., Dudhia, J., Gill, D.O., Barker. D.M., Duda, M.G., Huang, X.Y., Wang, W., and Powers, J.G. (2008) A Description of the Advanced Research WRF Version 3. NCAR Tech. Note NCAR/TN-475+STR, 113 pp. doi:10.5065/D68S4MVH.

Srinivas, C.V., Yesubabu, V., Prasad, D.H., Prasad, K.B.R.R.H., Greeshma, M.M., Baskaran, R., Venkataman, B. (2018) Simulation of an extreme heavy rainfall event over Chennai, India using WRF: sensitivity to grid resolution and boundary layer physics. Atmos. Res., pp. 66-82, 10.1016/j.atmosres.2018.04.014.

Shweta Bhati., and Manju Mohan. (2018) WRF-urban canopy model evaluation for the assessment of heat island and thermal comfort over an urban airshed in India under varying land use/land cover conditions. Geosci. Lett. ,5-28, https://doi.org/10.1186/s40562-018-0126-7.

Tao, W.K., Wu, D., Lang, S., Chern, J.D, Peters-Lidard, C., Fridlind, A., and Matsui, T. (2016) High-resolution NU-WRF simulations of a deep convective-precipitation system during MC3E: Further improvements and comparisons between Goddard microphysics schemes and obser- vations. J. Geophys. Res. Atmos., 121, 1278–1305.

Tewari, M., Chen, F., Wang, W., Dudhia, J., LeMone, M.A., Mitchell, K., Ek. M., Gayno, G.G., Wegiel, J., and Cuenca, R.H. (2004) Implementation and verification of the unified NOAH land surface model in the WRF model. 20th conference on weather analysis and forecasting/16th conference on numerical weather prediction, pp. 11–15.

Unnikrishnan, C.K., Gharai, B., Mohandas, S., Mamgain, A., Rajagopal, E.N., Gopal, R.I., and Rao, P.V.N. (2016) Recent change on land use/land cover over Indian region and its impact on the weather prediction using Unified model. Atmosp. Sci. Lett., doi:10.1002/asl.658.

Viswanadhapalli, Y., Challa, V.S., Basha, G., Dasari, H.P., Langodan, S., Venkat Ratnam, M., Hoteit I. (2019) A diagnostic study of extreme precipitation over Kerala during August 2018. Atmospheric Science Letters. doi: 10.1002/asl.941.

Wan, H.C., and Zhong, Z. (2014) Ensemble simulations to investigate the impact of large scale urbanization on precipitation in the lower reaches of Yangtze River Valley, China. Q. J. R. Meteorol. Soc., 140(678), 258– 266.

Yang, L., and Smith, J. (2018) Sensitivity of extreme rainfall to atmospheric moisture content in the arid/semiarid southwestern United States: Implications for probable maximum precipitation estimats. Journal of Geophysical Research: Atmospheres, 123, 1638–1656.

Yang, L., Tian, F.Q., Smith, J.A, and Hu, H.P. (2014) Urban signatures in the spatial clustering of summer heavy rainfall events over the Beijing metropolitan region. J. Geophys. Res. Atmos, 119, 1203– 1217.

Yatagai, A., Kamiguchi, K., Arakawa, O., Hamada, A., Yasutomi, N., and Kitoh, A. (2012) APHRODITE: Constructing a long-term daily gridded precipitation dataset for Asia based on a dense network of rain gauges. Bull. Am. Meteorol. Soc, 93, 1401–1415.

Yu, M., and Liu, Y. (2015) The possible impact of urbanization on a heavy rainfall event in Beijing. Geophys. Res. Atmos., 120, 8132-8143.

Zeng, X.M., Wu, Z.H., Song, S., Xiong, S.Y., Zheng, Y.Q., Zhou, Z.G., Liu, H.Q. (2012) Effect of land surface schemes on the simulation of a heavy rainfall event by WRF. Chin. J. Geophys, 55: 16–28.

Zhang, C.L., Chen, F., Miao, S.G., Li, Q.C., Xuan, C.Y. (2007) Influences of urbanization on precipitation and water resources in the metropolitan Beijing area. In Proceedings of the 21st American Metrological Society Conference on Hydrology, San Antonio, TX, USA.

Zhong, S., and Yang, X.Q. (2015) Ensemble simulations of the urban effect on a summer rainfall event in the Great Beijing Metropolitan Area. Atmos. Res., 153, 318– 334.

Table 1. List of LULC categories of ISRO and MODIS datasets.

S. No	**ISRO LULC categories**	**MODIS LULC categories**
1	Urban and Built-Up Land	Evergreen Needle leaf Forest
2	Dry land Cropland and Pasture	Evergreen Broadleaf Forest
3	Irrigated Cropland and Pasture	Deciduous Needle leaf Forest
4	Mixed Dry land/Irrigated Cropland and Pasture	Deciduous Broadleaf Forest
5	Cropland/Grassland Mosaic	Mixed Forests
6	Cropland/Woodland Mosaic	Closed Shrub lands
7	Grassland	Open Shrub lands
8	Shrub land	Woody Savannas
9	Mixed Shrub land/Grassland	Savannas
10	Savanna	Grasslands
11	Deciduous Broad leaf Forest	Permanent Wetlands
12	Deciduous Needle leaf Forest	Croplands
13	Evergreen Broad leaf	Urban and Built-Up
14	Evergreen Needle leaf	Cropland/Natural Vegetation Mosaic
15	Mixed Forest	Snow and Ice
16	Water Bodies	Barren or Sparsely Vegetated
17	Herbaceous Wetland	Water
18	Wooden Wetland	Wooded Tundra
19	Barren or Sparsely Vegetated	Mixed Tundra
20	Herbaceous Tundra	Barren Tundra
21	Wooded Tundra	
22	Mixed Tundra	
23	Bare Ground Tundra	
24	Snow or Ice	

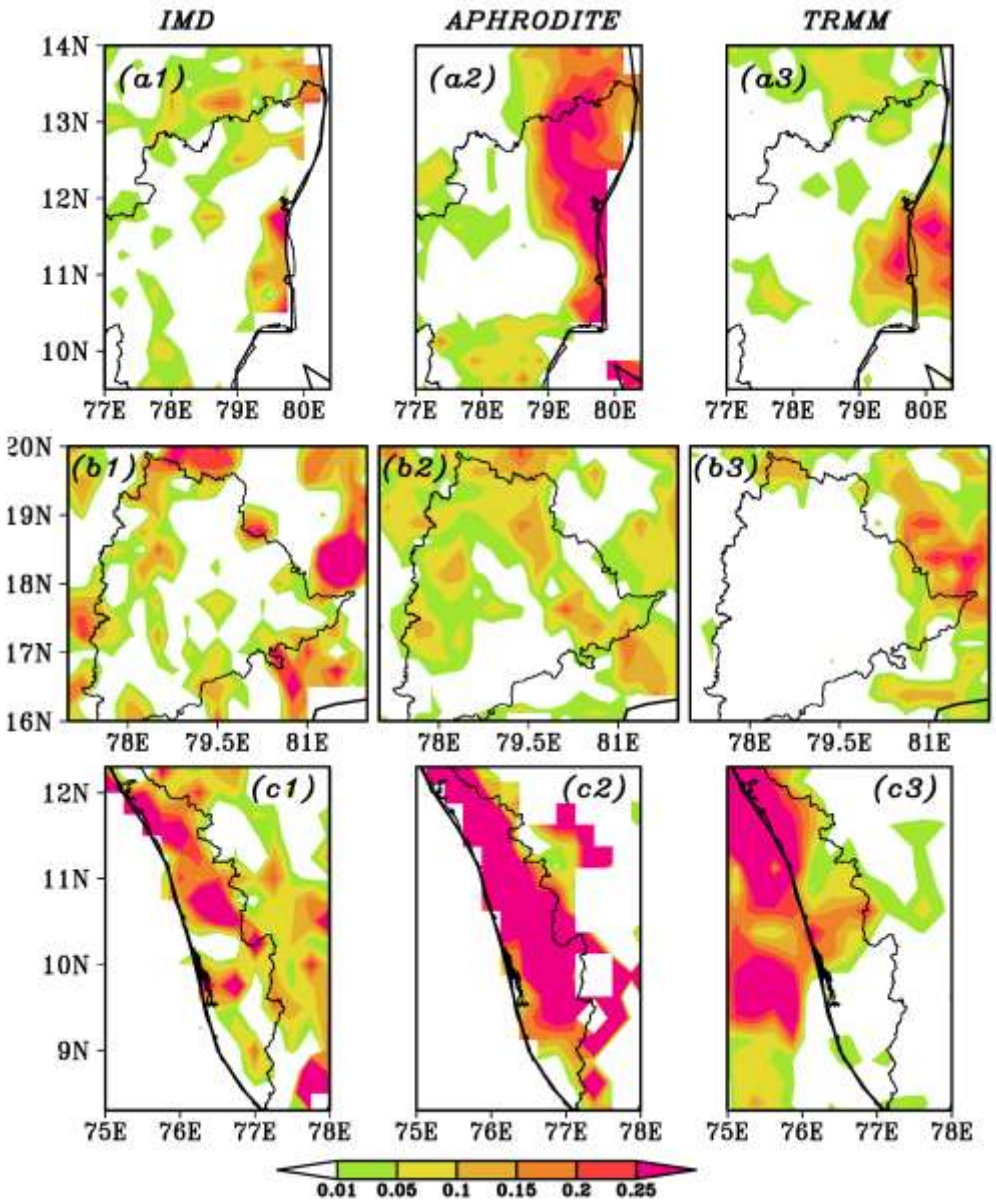

Figure 1. Spatial patterns of the linear trend in heavy rainfall days (those when the rainfall is ≥35.6 mm/day to ≤124.6 mm/day) during the OND season for Tamil Nadu, JJAS season for Telangana and Kerala for the period 2000-2017. Panels a1-a3, b1-b3, and c1-c3 are over Tamil Nadu, Telangana, and Kerala states, respectively. In all the three rows, the panels from left to right are based on the datasets from the IMD, APHRODITE and TRMM, respectively.

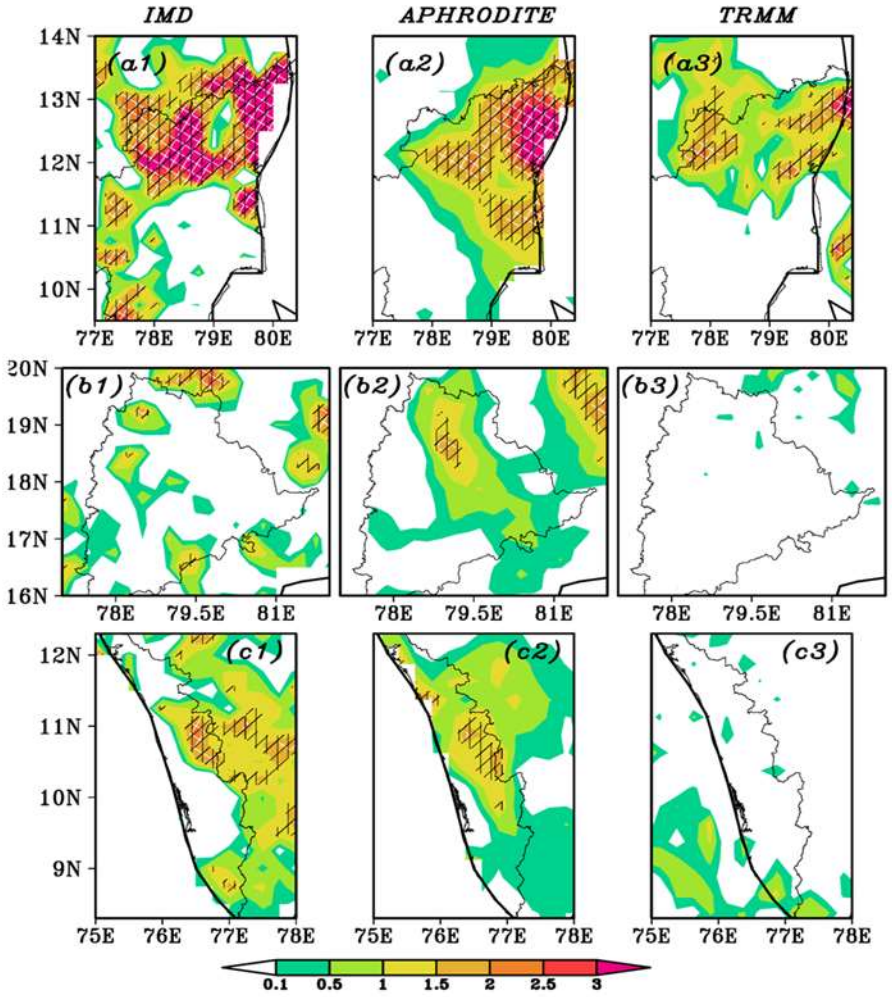

Figure 2. Same as Figure 1 but for the seasonal 99 percentile of rainfall magnitude. The white (black) color mesh shows the increasing trends at 95% (90%) confidence level.

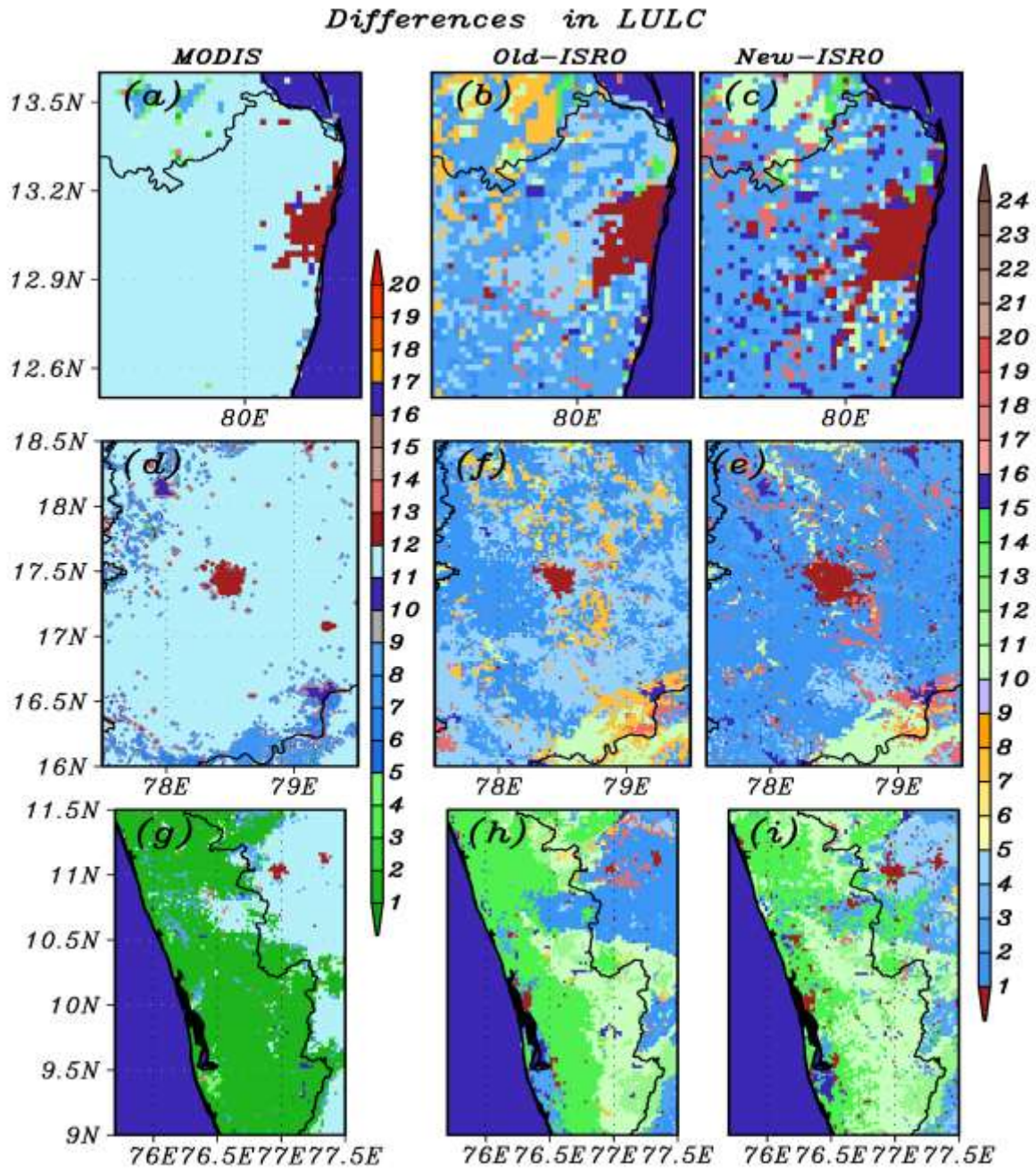

Figure 3. Spatial patterns of the LULC from three different datasets over three study regions. The regions shown are are, Tamil Nadu (top panels), Telangana (middle panels), and Kerala (lower panels). The LULC with MODIS is shown in the first column (a, d, and g), the Old-ISRO LULC for the year 2004-05 is shown in the second column (b, e, and h), and New-ISRO LULC for the year 2016-17 shown in the third column (c, f, and I). The urbanization of LULC=1 in ISRO and LULC=13 in MODIS.

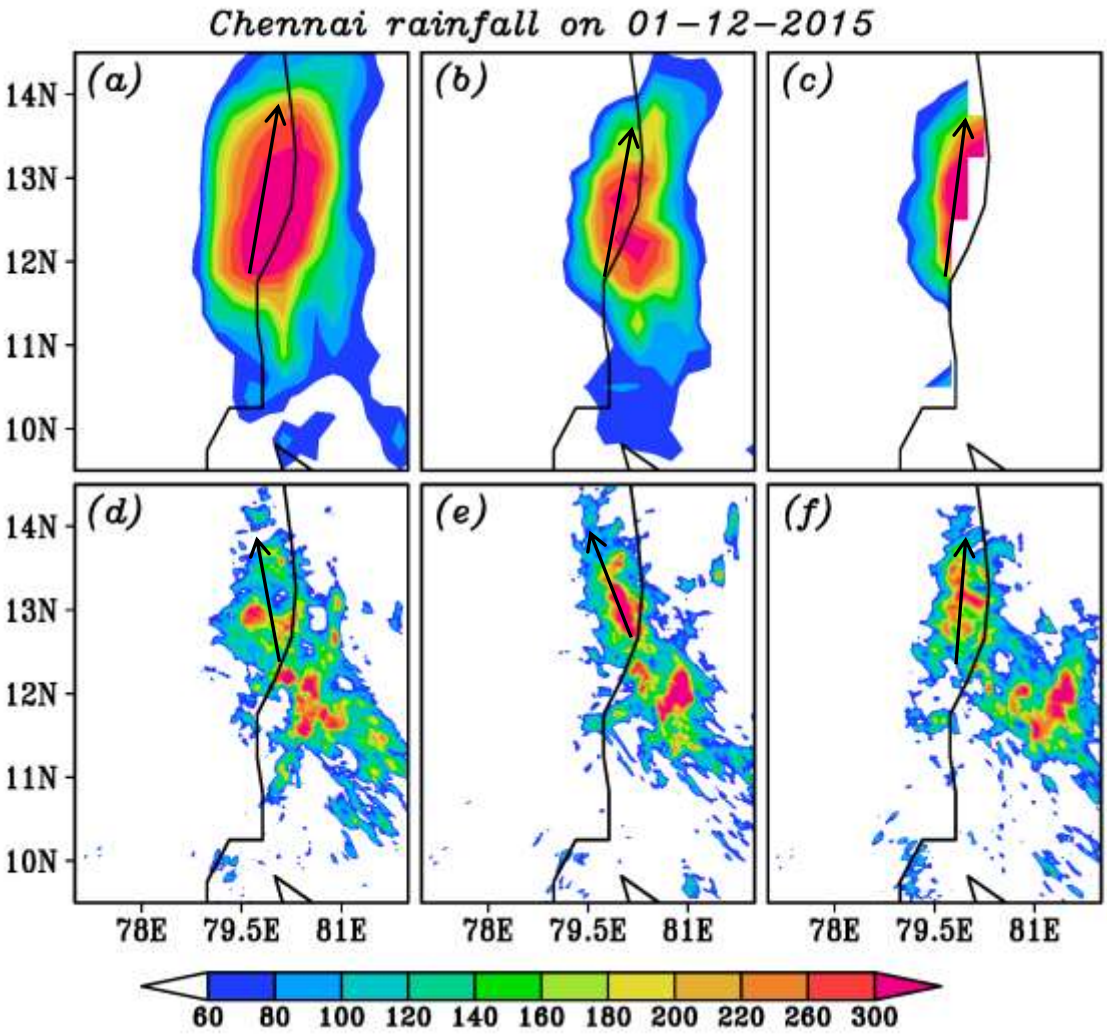

Figure 4. Spatial patterns of the rainfall over Tamil Nadu on 01-12-2015, during the Chennai heavy rainfall event. The first row shows the observed daily rainfall (mm/day) from (a) TRMM, (b) GPM-IMERG, and (c) IMD datasets. The second row shows the corresponding daily accumulated rainfall (mm/day) from the simulations with the LULC datasets of (d) MODIS, (e) Old-ISRO, and (f) New-ISRO. The arrows indicate the north-south orientation of the rainfall bands.

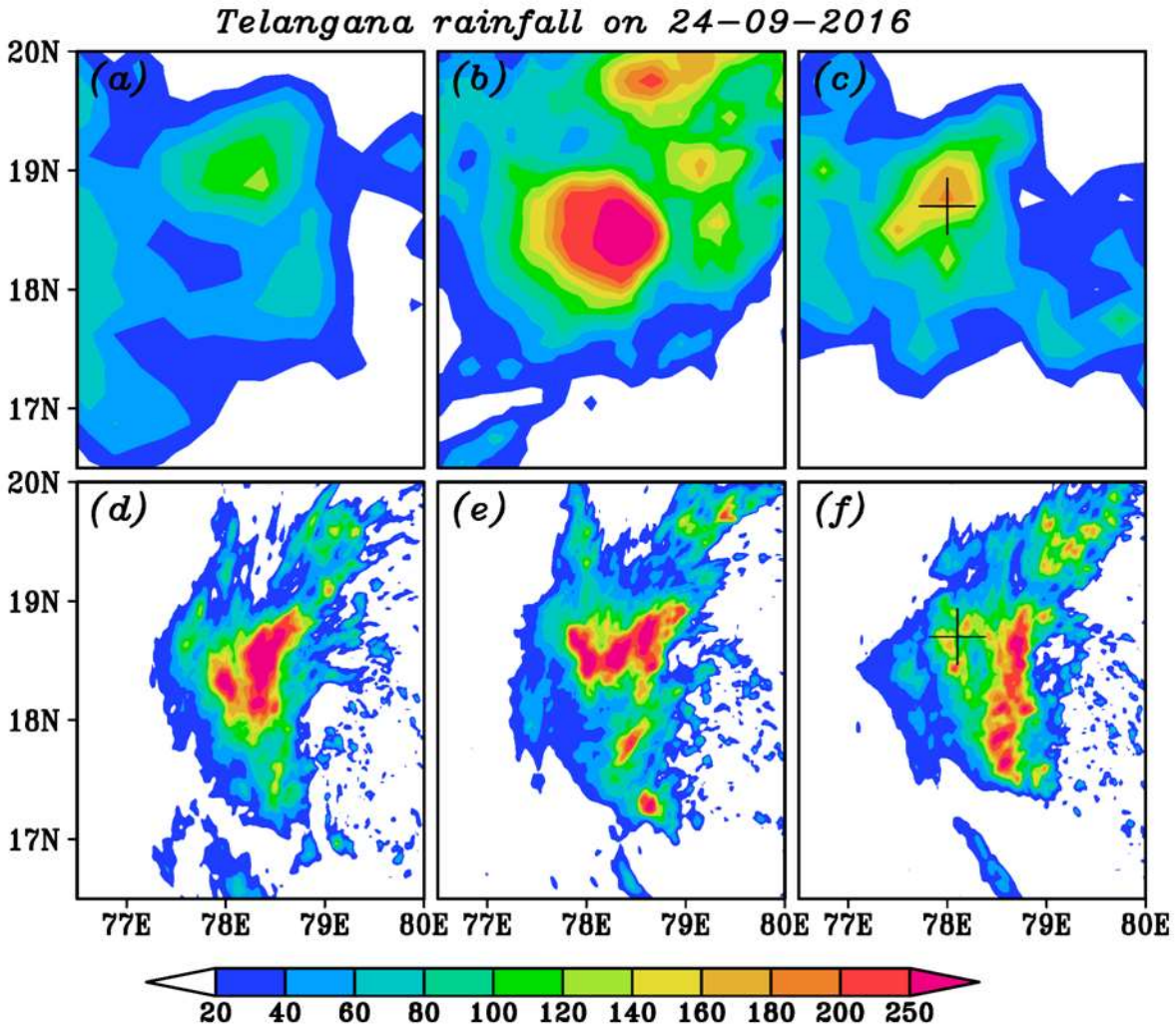

Figure 5. Same as Figure 4 but it is over Telangana, during the Telangana heavy rainfall event, on 24-09-2016. The plus (+) mark indicates the peak rainfall area in IMD observed and New-ISRO LULC simulated rainfall.

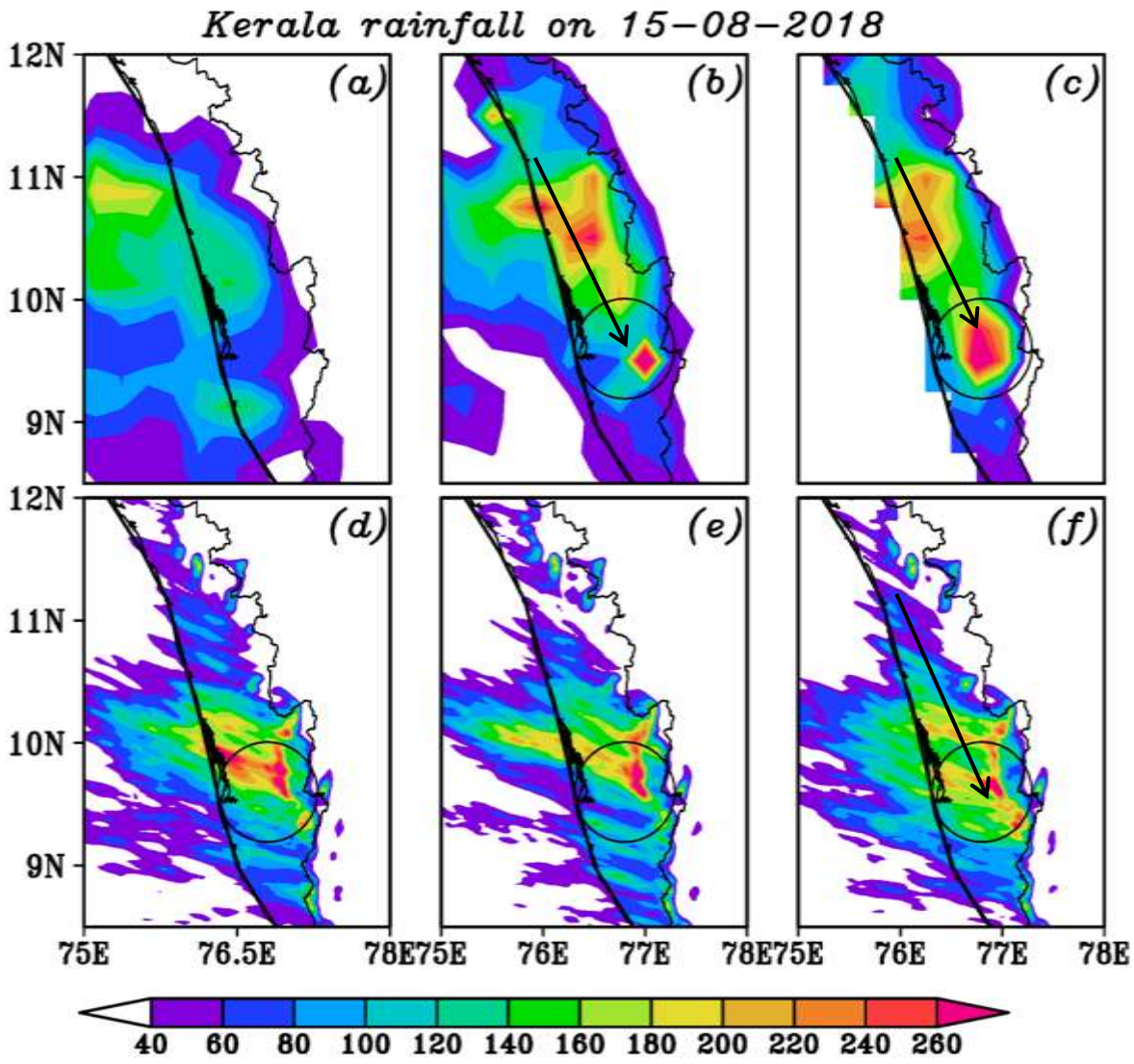

Figure 6. Same as Figure 4 but it is over Kerala, during the heavy rainfall event on 15-08-2018. The arrows indicate the northwest-southeast orientation of the rainfall band and the circle shows the high amount of rainfall concentrated area.

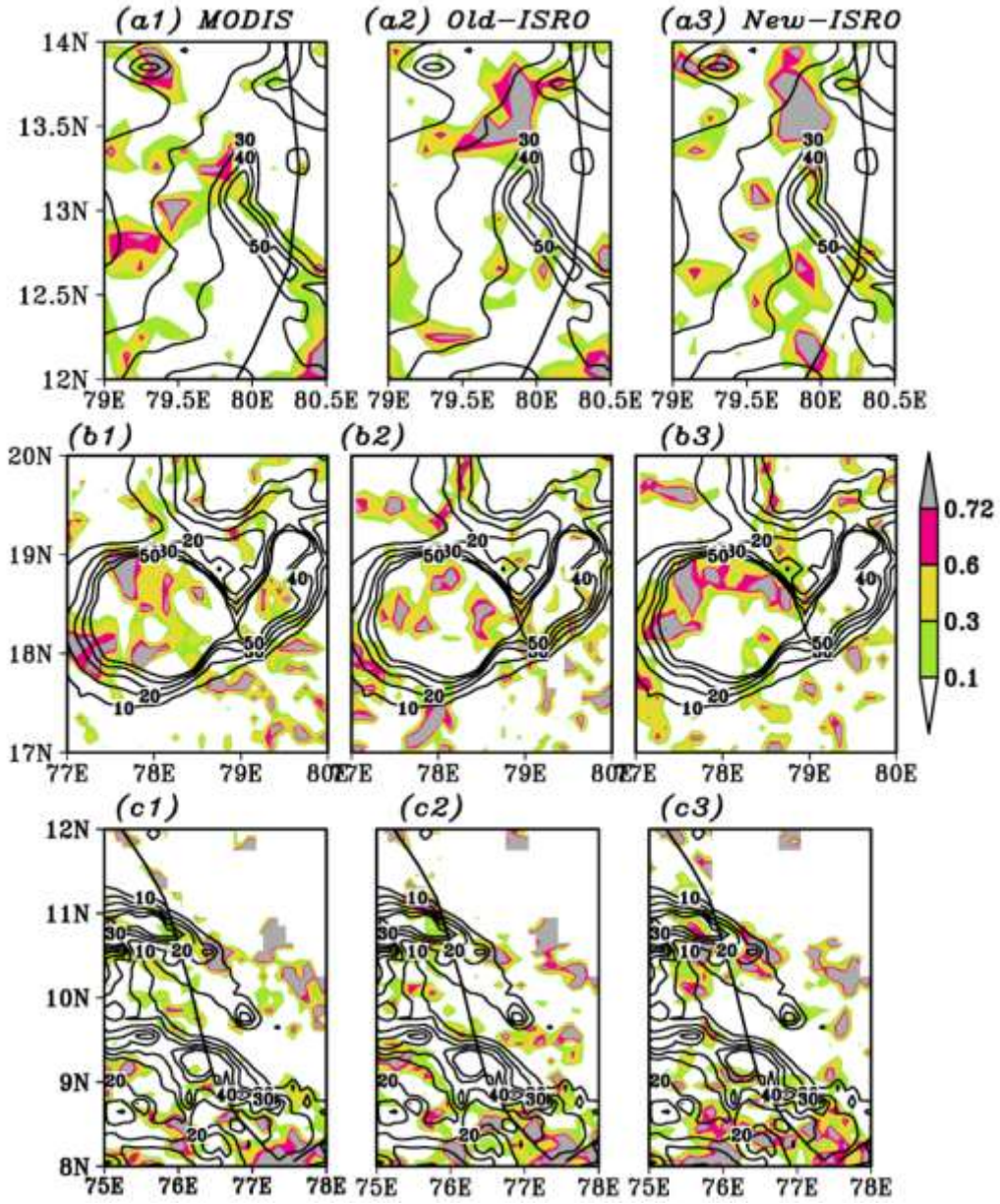

Figure 7. Correlation between the GPM-IMERG and model-simulated rainfall from the three experiments MODIS, Old-ISRO, and New-ISRO over Tamil Nadu (a1-a3), Telangana (b1-b3), and Kerala (c1-c3) during the eight rainfall hours. The shaded color shows the only the positive correlation values and the contour lines show the sum of eight rainfall (mm) hours from GPM-IMERG. The pink (gray) color indicates 90% (95%) confidence level from a one-tailed Student's t-test.

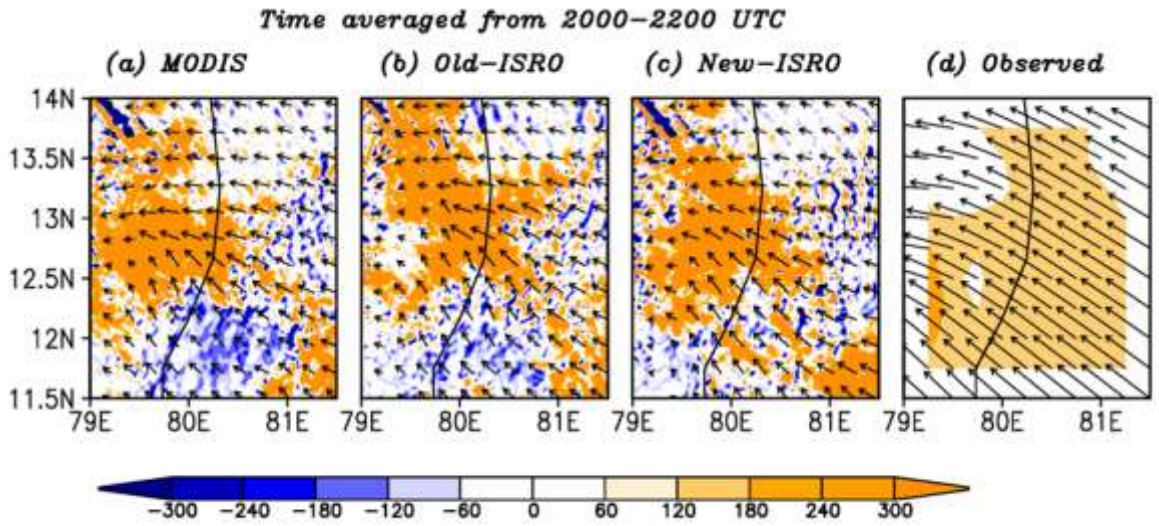

Figure 8. Spatial patterns of simulated vertically integrated moisture flux (10^{-6} kg m^{-2} s^{-1}) over Tamil Nadu during the Chennai heavy rainfall event. Positive and negative values indicate convergence and divergence, respectively. The wind vectors indicate moisture transport (kg m^{-1} s^{-1}). The panels (a), (b), (c), and (d) show results from simulations with the MODIS, Old-ISRO and New-ISRO LULC lower boundary conditions, and ERA5 observed datasets respectively, time averaged during the peak rainfall hours.

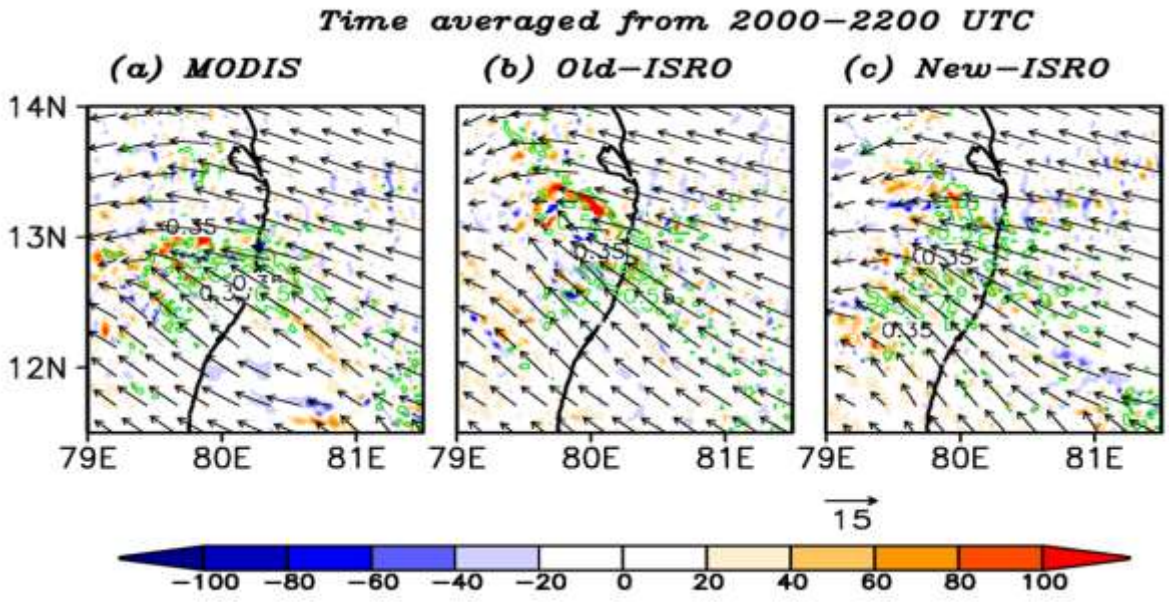

Figure 9. Spatial distribution of simulated vorticity (shaded), upward vertical wind (green contours) and zonal wind (vectors) at 850 hPa over Tamil Nadu during the Chennai rainfall event. The figures (a), (b), and (c) are from simulations with MODIS, Old-ISRO and New-ISRO LULC datasets, respectively, averaged during the peak rainfall hours.

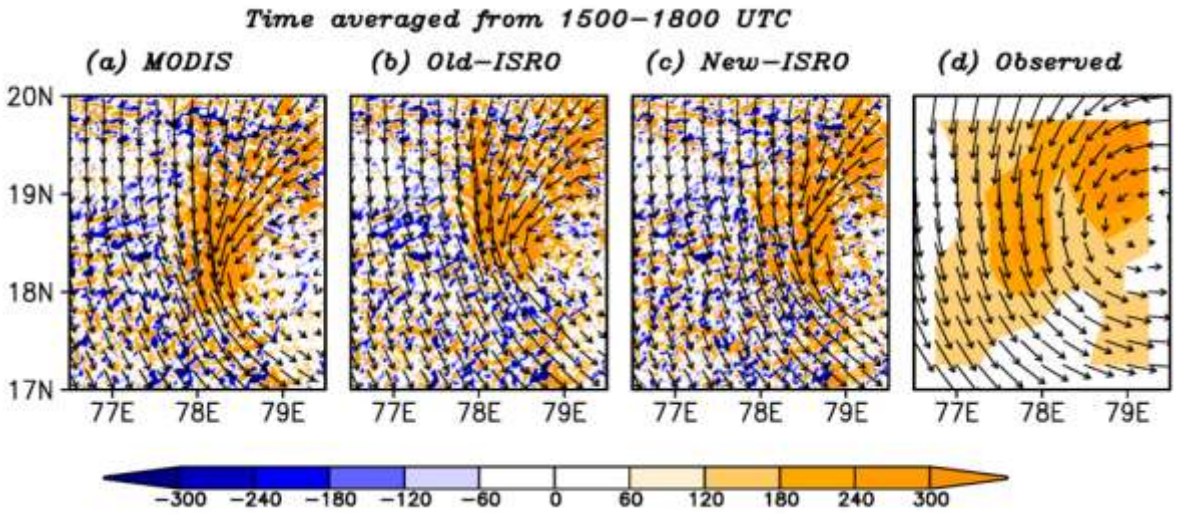

Figure 10. Same as Figure 8 but over Telangana during the Telangana heavy rainfall event.

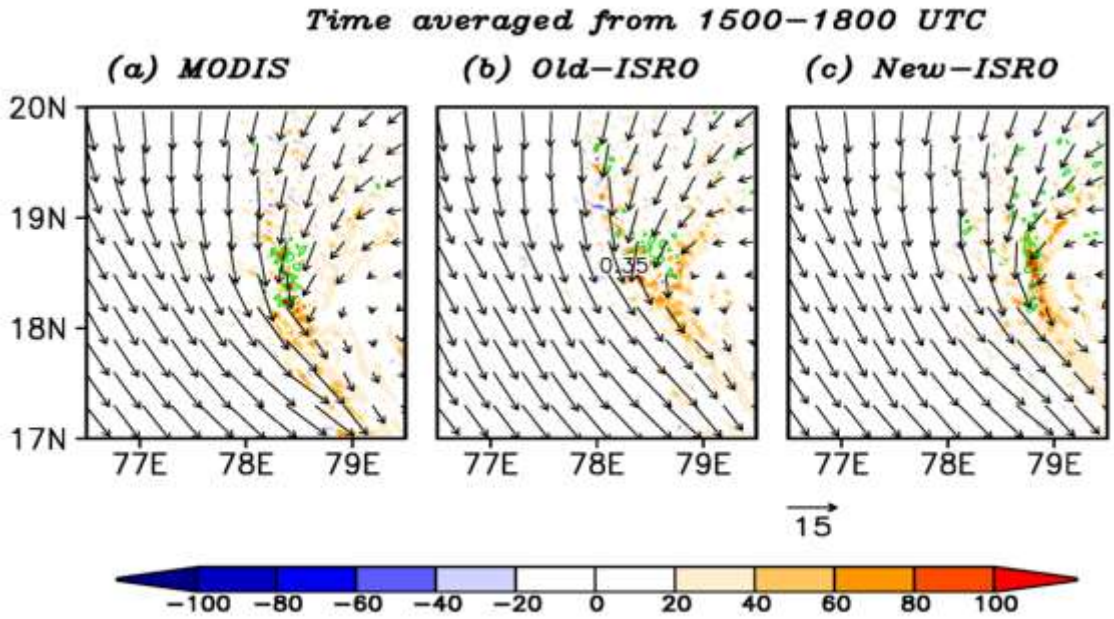

Figure 11. Same as Figure 9 but it is over Telangana during the Telangana heavy rainfall event.

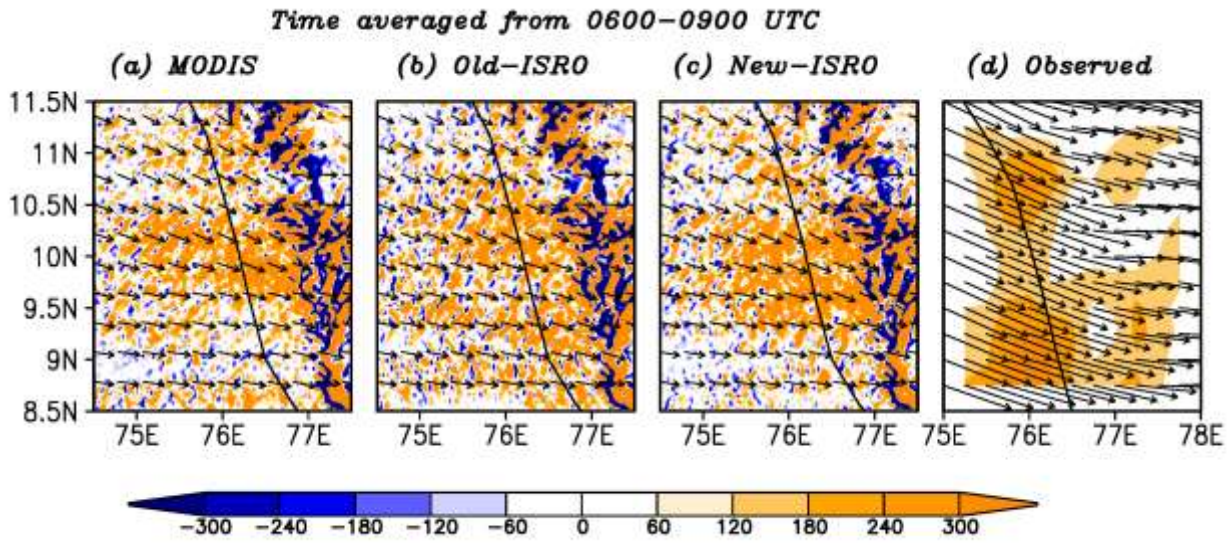

Figure 12. Same as Figure 8 but over Kerala during the Kerala heavy rainfall event.

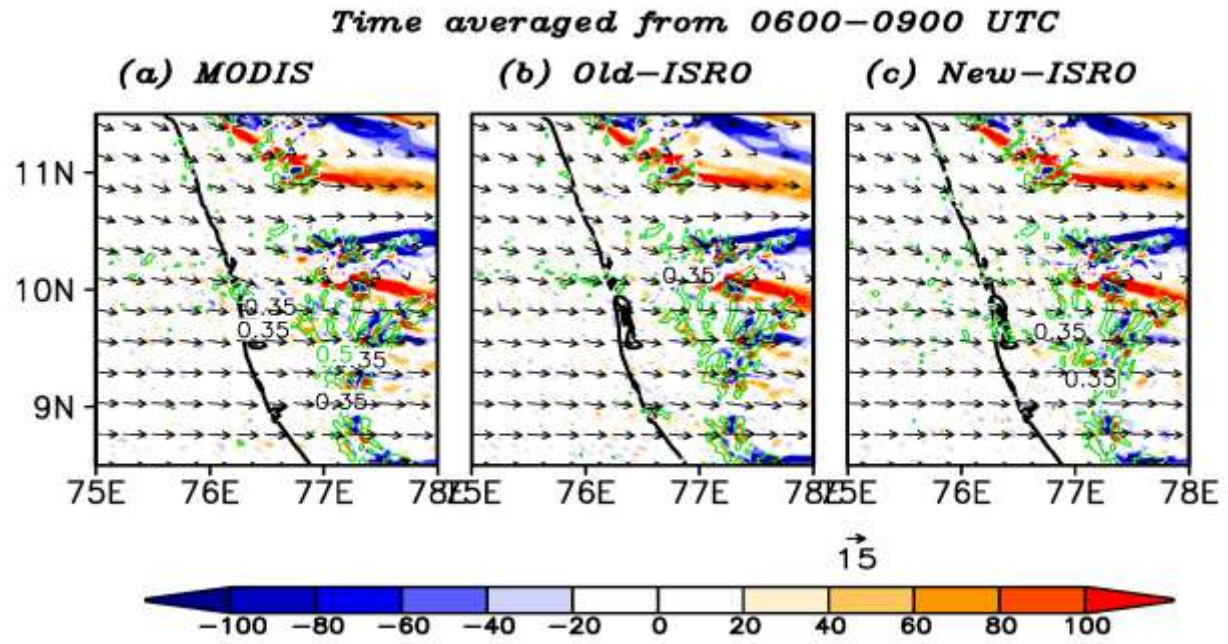

Figure 13. Same as Figure 9 but it is over Kerala during the Kerala heavy rainfall event.

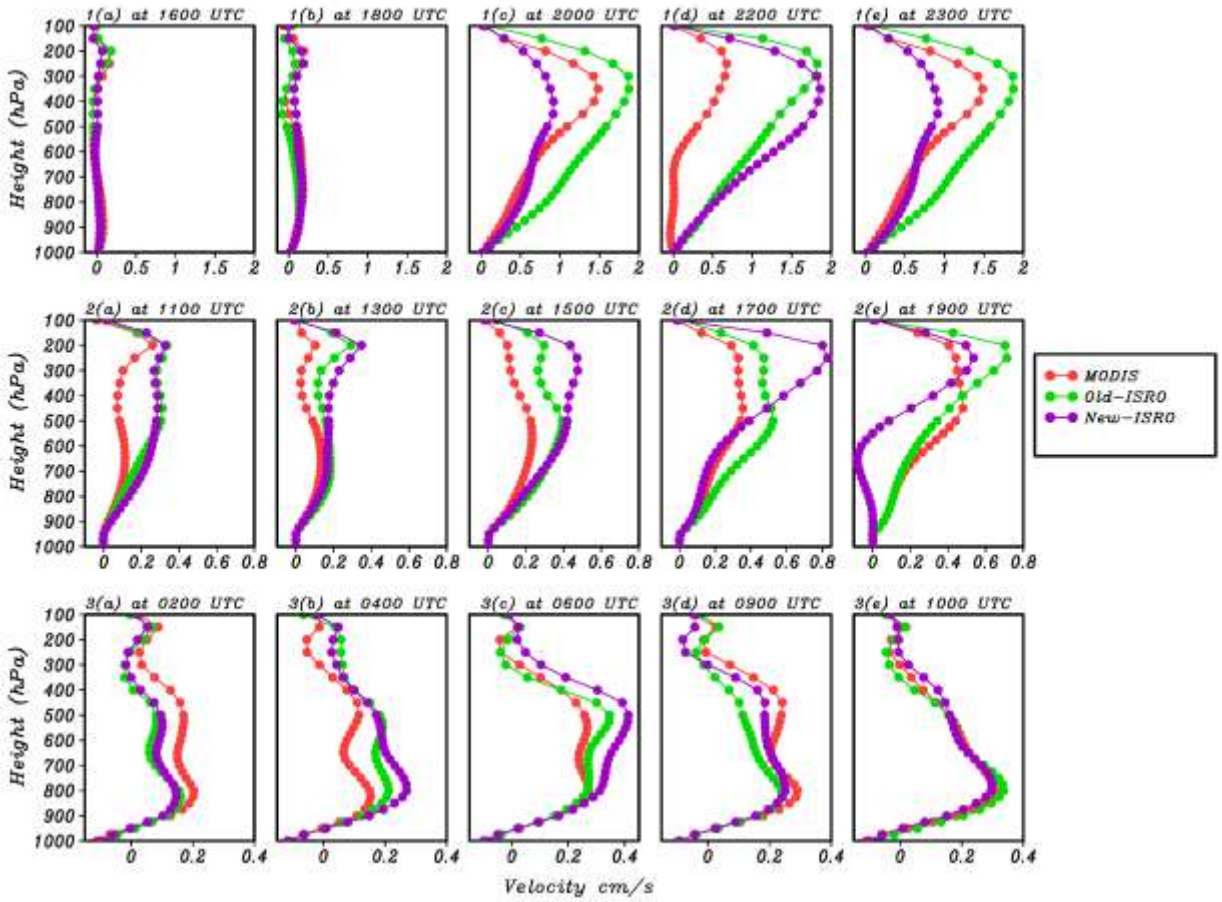

Figure 14. Area-averaged simulated vertical wind (cms^{-1}) profiles. The first row (1a-1e) pertains to the Chennai heavy rainfall event and values area-averaged over Tamil Nadu. The second (2a-2e) and third rows (3a-3e) are similar, but over Telangana and Kerala and pertain to respective representative events. The red, green and purple lines represent the simulations with MODIS, Old-ISRO and New-ISRO LULC lower boundary conditions, respectively. For a view of intra-stage evolution, these profiles are sampled twice during starting stage (1a-1b, 2a-2b, 3a-3b), thrice in peak (1c-1d, 2c-2d, 3c-3d), and thrice in decaying (1e, 2e, 3e) stages, respectively.

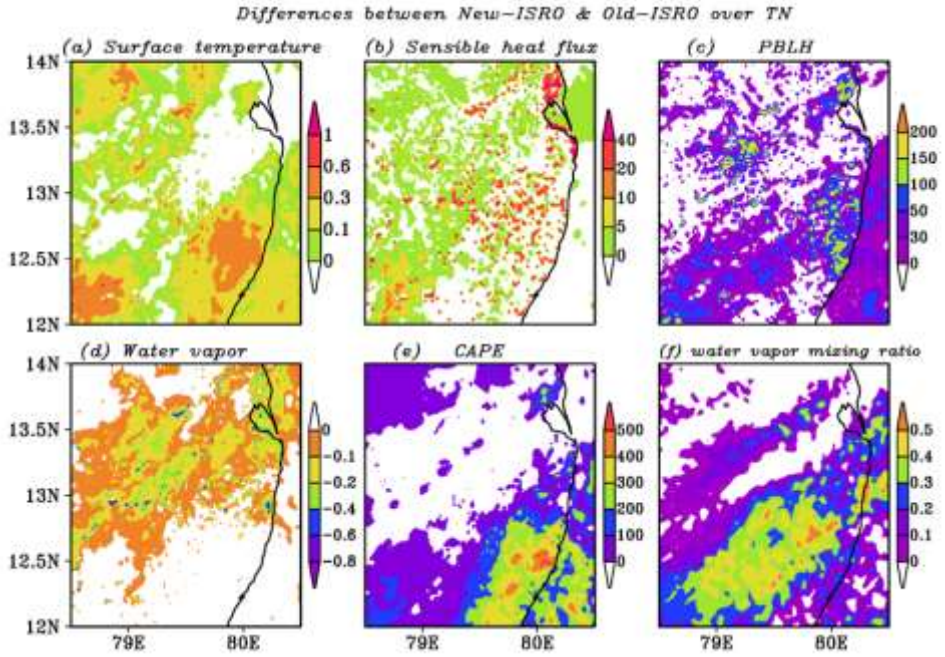

Figure 15. Difference plots over Tamil Nadu between Old-ISRO and New_ISRO LULC simulations, for the Chennai heavy rainfall event on 01-12-2015, of (a) surface temperature (°C), (b) sensible heat flux (W/m^2), (c) PBLH (m), (d) water vapor (g/kg), (e) CAPE (J/kg), and (f) water vapor mixing ratio (g/cm^2). The difference has been obtained by subtracting various parameters simulated in the experiment with the Old-ISRO LULC, from those from the corresponding New-ISRO LULC simulations.

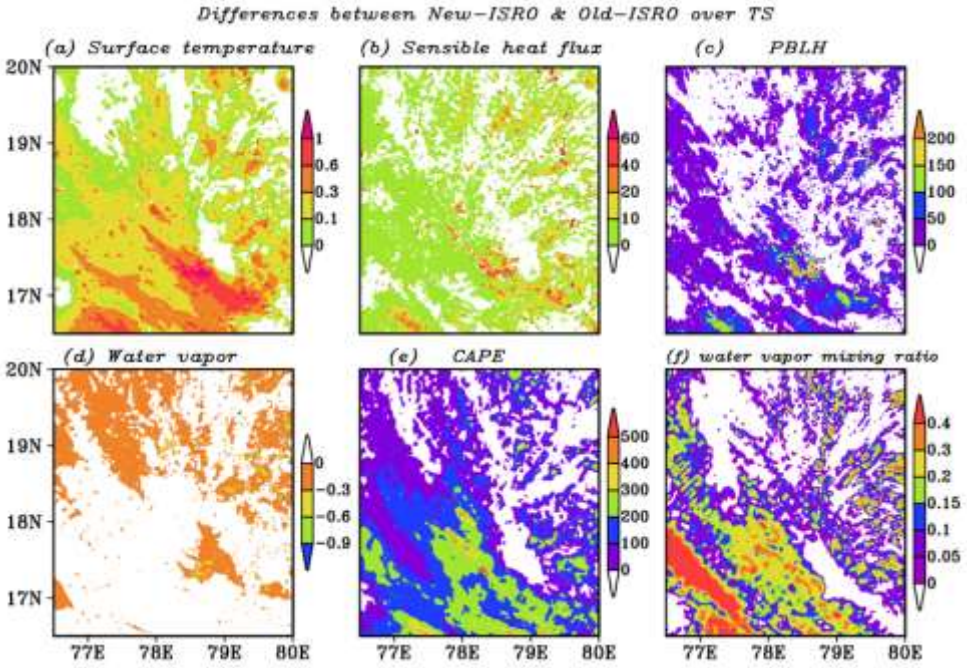

Figure 16. Same as Figure 15 but it is over Telangana, during the Telangana event on 24-09-2016.

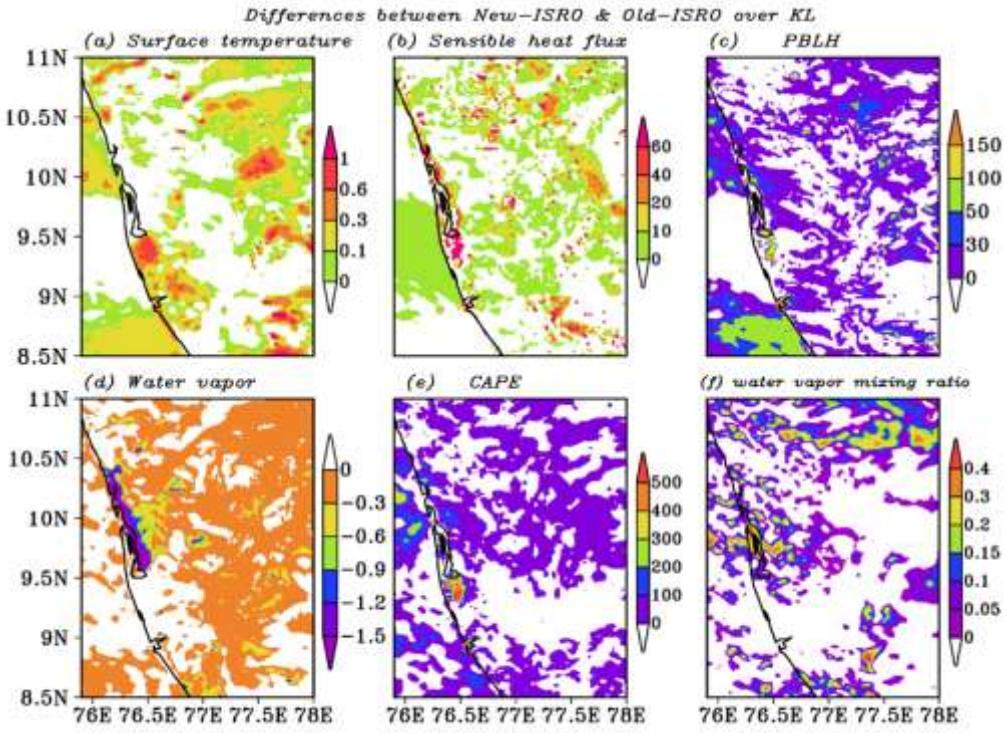

Figure 17. Same as Figure 15 but it is over Kerala, during the Kerala event on 15-08-2018.